Life-history strategies indicate live-bearing in *Nothosaurus* (Sauropterygia)

EVA M. GRIEBELER[1]* *and* NICOLE KLEIN[2,3]

[1]Institute of Organismic and Molecular Evolution, Evolutionary Ecology, Johannes Gutenberg-University, D-55099 Mainz, Germany

[2]State Museum of Natural History Stuttgart, Rosenstein 1, D-70191 Stuttgart, Germany

[3]Steinmann-Institute, Division of Palaeontology, University of Bonn, Nussallee 8, D-53115 Bonn, Germany

*Corresponding author: em.griebeler@uni-mainz.de

Contents

Text S1. Additional statistical analyses on differences in life-history strategies of extant oviparous and viviparous squamates that were presented in Hallmann & Griebeler (2015).

Text S2. Detailed description of our growth curve fitting method with a graphical representation of growth models applied.

Figure S1. Phylogenetic principal component analysis (pPCA) plot on oviparous and viviparous squamates (taken from Hallmann & Griebeler 2015, but modified).

Figure S2. Numbers of growth marks preserved by nothosaur specimens.

Figure S3. Birth to adult length ratios and numbers of clutches per year in extant squamates, and in viviparous fossils as well as in nothosaurs studied here and pachypleurosaurs studied by us before (Klein & Griebeler 2018).

Figure S4. Correlation between humerus length and snout-vent-length in extant squamates.

Figure S5. Relationship between birth-to-adult size ratio and clutch size in extant squamates and nothosaur birth-to-adult size ratios.

Figure S6. Growth record traced in *Nothosaurus* humeri Wijk13-141, Wijk11-20, MHI 1193, and GPIT/R/1339d.

Figure S7. Growth record traced in *Nothosaurus* humeri MB.R 162.4, MHI 1978, and SMNS 84851.

Figure S8. Growth record traced in *Nothosaurus* humeri SMNS 7175, SMNS 84772, MB.R. 272, MB. R. 282, and StIPB R 45.

Figure S9. Growth record traced in *Nothosaurus* humerus MB.R. 269, and *Ceresiosaurus* humerus PIMUZ T4845.

Table S1. Growth records and models for a) early Anisian (Lower Muschelkalk), b) middle to late Anisian (Middle Muschelkalk), and c) latest Anisian to early Ladinian (Upper Muschelkalk) *Nothosaurus* humeri studied.

Table S2. Life-history traits and birth to adult length ratios derived from best growth models for 24 *Nothosaurus* specimens from the early Anisian to late Ladinian (Middle Triassic; lithostratigraphical units: Lower Muschelkalk, Middle Muschelkalk and Upper Muschelkalk).

Table S3. Information on birth to adult size ratios and clutch sizes of fossil taxa for which viviparity is inferred from or documented in the fossil record.

Table S4. Life-history traits and birth-to-adult length ratios derived from best growth models established for pachypleurosaur specimens studied in Klein & Griebeler (2018).

Text S1.

The study of Hallmann & Griebeler (2015) inferred differences in six life-history traits of oviparous and viviparous squamate species using phylogeny-informed principle component analysis (pPCA). Their pPCA clearly mapped viviparous species in the upper left quadrant (for convenience their plot is shown here again in fig. S1), whereas oviparous species were distributed all over the plot. Their plot thus suggests differences in life-history strategies of both species groups. In their Supporting Information the authors also conducted pPCA for five life-history traits of more than 300 squamate species using the Scharf *et al.* (2015) dataset. Although the latter pPCA did not use information on incubation/gestation time of species, it corroborated the first in terms of differences in the other five life-history traits between oviparous and viviparous species.

In the following, we provide additional statistical analyses (carried out in STATISTICA 10, Statsoft Inc. 2011) in order to strengthen their observed differences in life-history traits between oviparous and viviparous species because this study on *Nothosaurus* makes use of these differences. We carried out the new analyses with the small dataset analysed in Hallmann & Griebeler (2015). It consists of 32 squamate species of which seven are viviparous and 25 are oviparous (HG dataset). The HG dataset provides information on asymptotic age/maximum longevity (years), age at which females are sexually mature (days), total length at birth (cm), number of eggs/litter size per clutch, number of clutches per year, incubation time (days), and adult body weight (g) of species. As the HG dataset is comparatively small, we also analysed the dataset from Scharf *et al.* (2015) (S dataset) again. The S dataset provides only information on five traits, but has an order of magnitude more species than the HK dataset. Traits covered by the S dataset are maximum longevity (years), age at maturity (months), hatchling mass (g), number of eggs/litter size per clutch, and number of clutches per year.

Hallmann & Griebeler (2015) concluded from their pPCA (fig. S1) that on average viviparous squamates reach later sexual maturity, produce fewer and larger clutches, have a longer gestation/incubation time, are larger at birth, and have a considerable larger maximum longevity when compared to oviparous squamate species. The following Table A shows for each of these life-history traits the results of U-tests carried out on the viviparous

and oviparous squamates from the HG and the S dataset, respectively. U-tests corroborate at the median level all differences in life-history traits between oviparous and viviparous species that are reported in Hallmann & Griebeler (2015).

Table A. Differences in life-history traits between extant oviparous and viviparous squamates. Results of U-tests carried out for A) 32 extant squamate species from Hallmann & Griebeler (2015, HG dataset), and B) for extant squamates from Scharf *et al.* (2015, S dataset).

Trait A) HG dataset	$N_{oviparous}$	$N_{viviparous}$	Oviparous species Median (Range)	Viviparous species Median (Range)	U	p
Birth size (total length, cm)	25	7	7.56 (2.05, 33.83)	16.75 (4.53, 19.70)	54.0	0.135
Female maturity (days)	25	7	730.00 (240.00, 1824.50)	1156.00 (6.95, 1825.00)	58.5	0.191
Maximum longevity (years)	25	7	13.00 (2.50, 24.25)	19.00 (7.50, 44.33)	63.5	0.281
Clutch size	25	7	6.00 (1.5, 21.67)	11.33 (5.67, 14.16)	45.5	0.054
Number of clutches per year	25	7	1.5 (1.00, 6.00)	1.00 (0.69, 2.00)	40.5	**0.030**
Incubation time (days)	25	7	56.94 (40.00, 99.25)	90.00 (74.00, 107.00)	16.0	**<0.001**
B) S dataset						
Birth size (mass, g)	577	204	0.90 (0.05, 320.75)	2.90 (0.08, 310.00)	41344.5	**$<10^{-8}$**
Female maturity (months)	319	92	16.75 (1.00, 144.00)	30.00 (5.50, 84.00)	8188.5	**$<10^{-10}$**
Maximum longevity (years)	731	283	8.25 (0.50, 91.00)	12.50 (1.25, 54.00)	77193.5	**$<10^{-9}$**
Clutch size	682	258	5.00 (1.00, 87.00)	7.00 (1.00, 51.00)	69161.0	**$<10^{-6}$**
Number of clutches per year	402	136	1.50 (0.22, 25.50)	1.00 (0.38, 3.00)	9021.0	**$<10^{-16}$**

To find out whether life-history trait combinations can indeed discriminate oviparous and viviparous squamate species we further conducted linear discriminant analysis (LDA) for both the HG and S dataset (Table B). We considered in different LDAs a stepwise increasing number of traits (three up to five/six) potentially discriminating oviparous and viviparous species. Please note that birth size, age at sexual maturation, and asymptotic size are inferable for nothosaur specimens from growth curves. We were able to take into consideration nothosaur clutch/litter size by estimating these from their birth-to-adult size ratio. Numbers of clutches per year are independent of the birth-to-adult size ratio in extant squamates

and were thus not estimated for nothosaurs. For both the HG and S dataset Wilk's λ decreases and canonical R values increase with an increasing number of traits used in the LDA.

Table B. Linear discriminant analyses (LDA) on different sets of life-history traits for A) 32 extant squamate species from Hallmann & Griebeler (2015, HG dataset), and B) extant squamates from Scharf *et al.* (2015, S dataset). LDAs were carried out with standardized values of life-history traits. For trait standardization we applied the formula ((trait value – mean of trait values)/variance of trait values) with the mean and variance of each trait calculated from the 32 squamate species and all squamates from Scharf *et al.* (2015), respectively. When using the large S dataset birth size, female maturity, and maximum longevity can already discriminate oviparous and viviparous squamates. Adding clutch size and even number of clutches per year only slightly increases again the discrimination power in terms of Wilk's λ and canonical R. This pattern is also observed for the smaller HG dataset, although for this Wilk's λ is only significant when six traits are used. The small HG dataset indicates that incubation/gestation time is an important discriminator on the reproduction mode in extant squamates. In the model that includes all six traits, Wilk's λ is nearly halved and the canonical R value is more than doubled compared to all models without this trait. Unfortunately, incubation/gestation time is unpreserved in fossils. Please note the different units of traits birth size and female maturity in A) and B). In A) birth size = total length at birth in cm and female maturity is given in days. In B) birth size = hatchling/birth mass in grams and female maturity is given in months.

Traits A) HG dataset	$N_{oviparous}$	$N_{viviparous}$	Wilk's λ	F	p	Mahalanobis distance	Canonical R
Birth size + Female maturity + Maximum longevity	25	7	0.899	1.047	0.387	0.616	0.318
Birth size + Female maturity + Maximum longevity + Clutch size	25	7	0.846	1.228	0.322	0.998	0.392
Birth size + Female maturity + Maximum longevity + Clutch size + Number of clutches per year	25	7	0.805	1.252	0.314	1.321	0.441
Birth size + Female maturity + Maximum longevity + Clutch size + Number of clutches per year + Incubation time	25	7	0.459	4.941	**0.002**	6.470	0.735
B) S dataset							
Birth size + Female maturity + Maximum longevity	294	84	0.950	6.488	**<0.001**	0.300	0.223
Birth size + Female maturity + Maximum longevity + Clutch size	290	84	0.950	4.822	**<0.001**	0.300	0.223
Birth size + Female maturity + Maximum longevity + Clutch size + Number of clutches per year	265	76	0.915	6.217	**$<10^{-4}$**	0.533	0.291

For the S dataset differences in Mahalanobis distances predicted by LDAs with three up to five traits differed significantly between oviparous and viviparous species, for the HG dataset this distance was only significant when six traits were used (Figure A). Overall, LDAs statistically proved the differences in life-history strategies of extant squamates that Hallmann & Griebeler (2015) elaborated with pPCA and that we used in this study to assess the reproduction mode of nothosaurs.

Figure A. Canonical values obtained from linear discriminant analysis (LDA) on life-history strategies for A) 32 extant squamate species from Hallmann & Griebeler (2015, HG dataset), and B) extant squamates from Scharf *et al.* (2015, S dataset). Means, standard deviation and range of canonical values of viviparous and oviparous squamate groups (one-dimensional, two groups) are shown. Arrows indicate standardized canonical variables (life-history traits) of LDA models (three up to five/six life-history traits, from left to right). D = Mahalanobis distance between the viviparous and oviparous squamate group, p values indicate significance of D. For further information and results on each LDA refer to Table B. Life-history traits used in LDAs: birth size = total length at birth in A) and hatchling/birth mass in B), maturity = age at which females reach sexual maturity (in A the unit is days and in B it is months), longevity = maximum longevity, clutch size = number of eggs/litter size, # clutches = number of clutches per year, and incubation = incubation time.

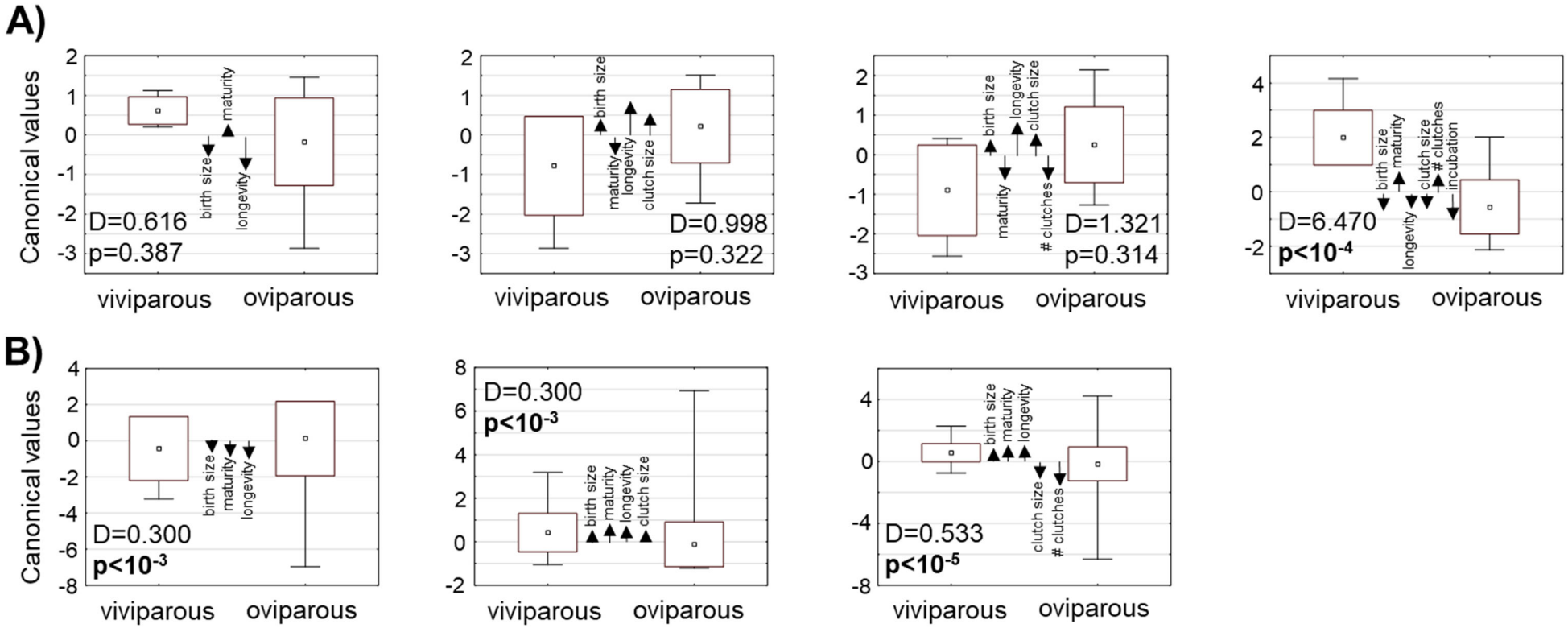

In principle, LDA is able to classify other observations into analysed groups. Thus, for our nothosaur sample it would be straightforward to do this based on the discriminant functions derived from the S dataset. However, the S dataset provides hatchling/birth mass (g) as a measure of birth size, whereas for nothosaur specimens masses are unknown and we had to use midshaft width at sampling location (and to estimate humerus length from width for a comparison of nothosaur and pachypleurosaur life-history strategies) as a proxy of individual size (see main text). Because information on midshaft width and on humerus length of extant squamates is rare (see fig. S4) we applied a PCA approach to identify potentially viviparous

nothosaur specimens. The following Figure B demonstrates that PCAs and LDAs carried out for extant squamates reveal rather similar results in terms of discrimination of squamate reproduction modes.

Figure B. Comparison of results of principle component analyses (PCA) and linear discriminant analyses (LDA) on different life-history traits of extant squamates. Squamate life-history traits were taken from Scharf *et al.* (2015, S dataset). A) PCA and LDA results on three traits (birth size, female maturity, maximum longevity), B) PCA and LDA results on four traits (birth size, female maturity, maximum longevity, clutch size), and C) PCA and LDA results on five traits (birth size, female maturity, maximum longevity, clutch size, number of clutches per year). Arrows in the LDA subpanels are standardized canonical variables obtained for the respective life-history trait dataset. PCAs and LDAs were carried out with standardized values of life-history traits. For standardization of traits we applied the formula ((trait value – mean of trait values)/variance of trait values) with the mean and variance of each trait calculated from all squamate species of the dataset. For more information on LDAs refer to Table B and Figure A. PCA and LDA reveal a similar ordination/discrimination of squamate species with respect to their life-history strategy. In PCA A) through C), female maturity and maximum longevity always correlate highly. Both traits are the largest canonical factors in the respective LDAs. When adding birth size to female maturity and maximum longevity (A), birth size adds to the explanation of the overall variability in squamate life-history strategies. The latter is consistent with a moderate value of this canonical variable compared to female maturity and maximum longevity (A). However, the adding of birth size in the PCA is less informative when clutch size is also included (B). Birth size now correlates more with female maturity and maximum longevity than in (A), and in the LDA the value of the canonical value of birth size decreases. The trait number of clutches per year correlates negatively with clutch size (C). In the LDA, their negative correlation is reflected by a negative value of this trait and a positive value of clutch size (C). Abbreviations of life-history traits: birth size = total length at birth or hatchling/birth mass, maturity = age at which females reach sexual maturity, longevity = maximum longevity, clutch size = number of eggs/litter size, # clutches = number of clutches per year, and incubation = incubation time.

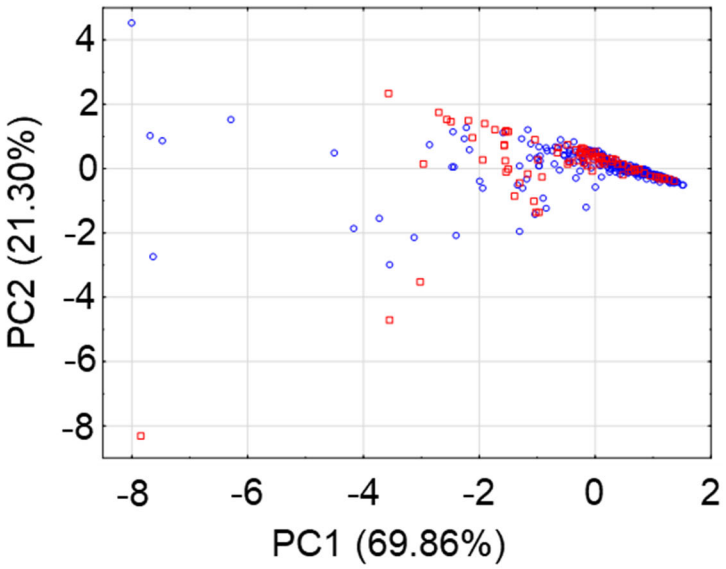

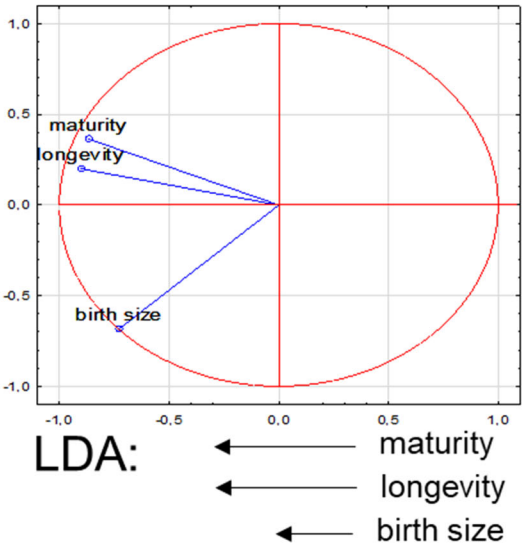

LDA: maturity, longevity, birth size

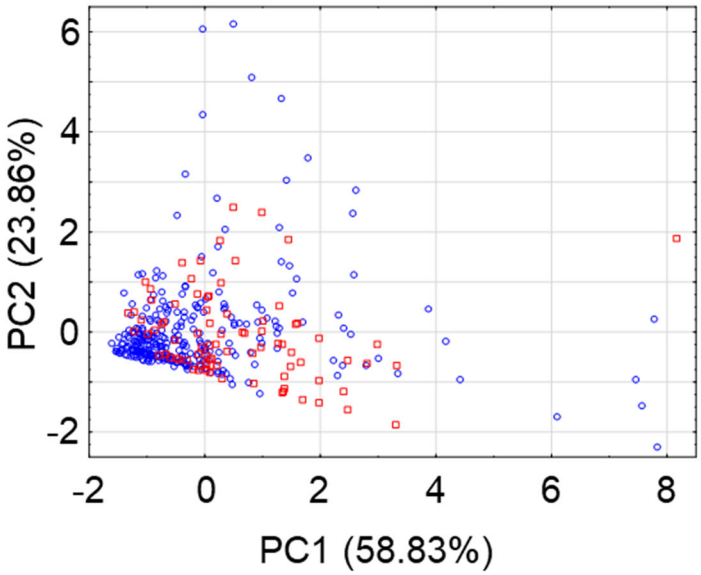

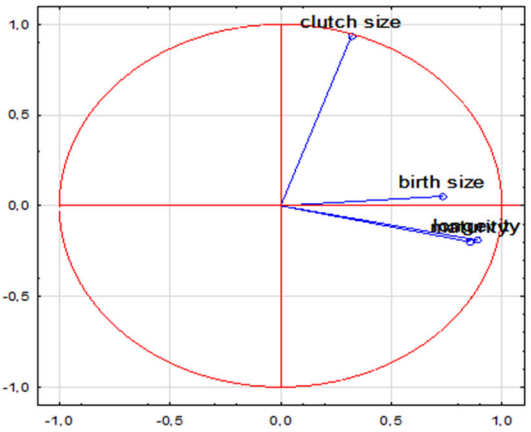

LDA: maturity, longevity, birth size, clutch size

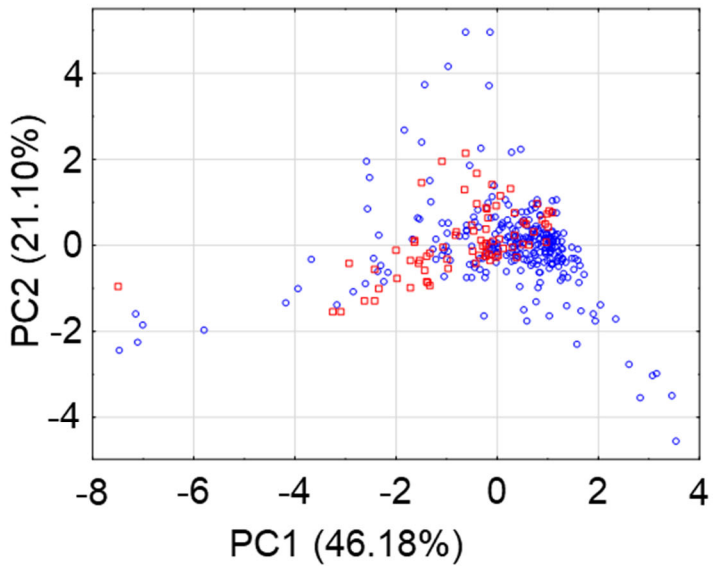

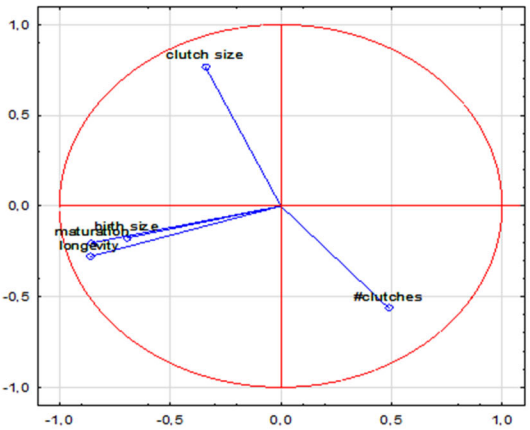

LDA: maturity, longevity, birth size, clutch size, #clutches

As the phylogeny of nothosaur specimens analysed by us is unclear, we used non-phylogeny-informed statistics throughout our study. Using phylogeny-informed analysis only for extant squamates and comparing it to non-phylogeny-informed analysis on nothosaurs (and pachypleurosaurs) would be inappropriate, as phylogeny- and non-phylogeny-informed results are not comparable. Figure C shows the results of PCA and pPCA conducted for both the HG and S dataset. While for the small HG dataset PCA and pPCA results differ in terms of life-history trait vectors (length and angle), they do much less for the large S dataset. Nevertheless, the mapping of viviparous squamates is consistent under the PCA and pPCA even when the small HG dataset is used.

Figure C. Comparison of non-phylogeny-informed and phylogeny-informed principal component analysis on squamate life-history strategies. Hallmann & Griebeler (2015) conducted phylogeny-informed PCA (pPCA) on 32 squamate species using six traits (birth size, clutch size, number of clutches per year, incubation time, female maturity, maximum longevity, HG dataset) and for the squamate species from Scharf *et al.* (2015) using five traits (birth size, clutch size, number of clutches per year, incubation time, female maturity, maximum longevity, S dataset). In this study, we conducted non-phylogeny-informed principal component analysis (PCA). A) PCA and pPCA results on 32 squamate species, and B) PCA and pPCA results on squamates from Scharf *et al.* (2015). Please note that in the plots of the pPCAs taken from Hallmann & Griebeler (2015) three categories are marked (oviparity with rigid-shelled eggs +, oviparity with parchment-shelled eggs Δ, viviparity ●) while in the plots on the non-phylogeny-informed PCAs only two categories are marked (oviparity Δ, viviparity ●) and that in the pPCA in B) hatchling mass is used, whereas the respective PCA is based on the total length at birth. PCAs and pPCAs differ more for the smaller dataset than for the large one. Numbers of species of the HG dataset as in fig. S1.

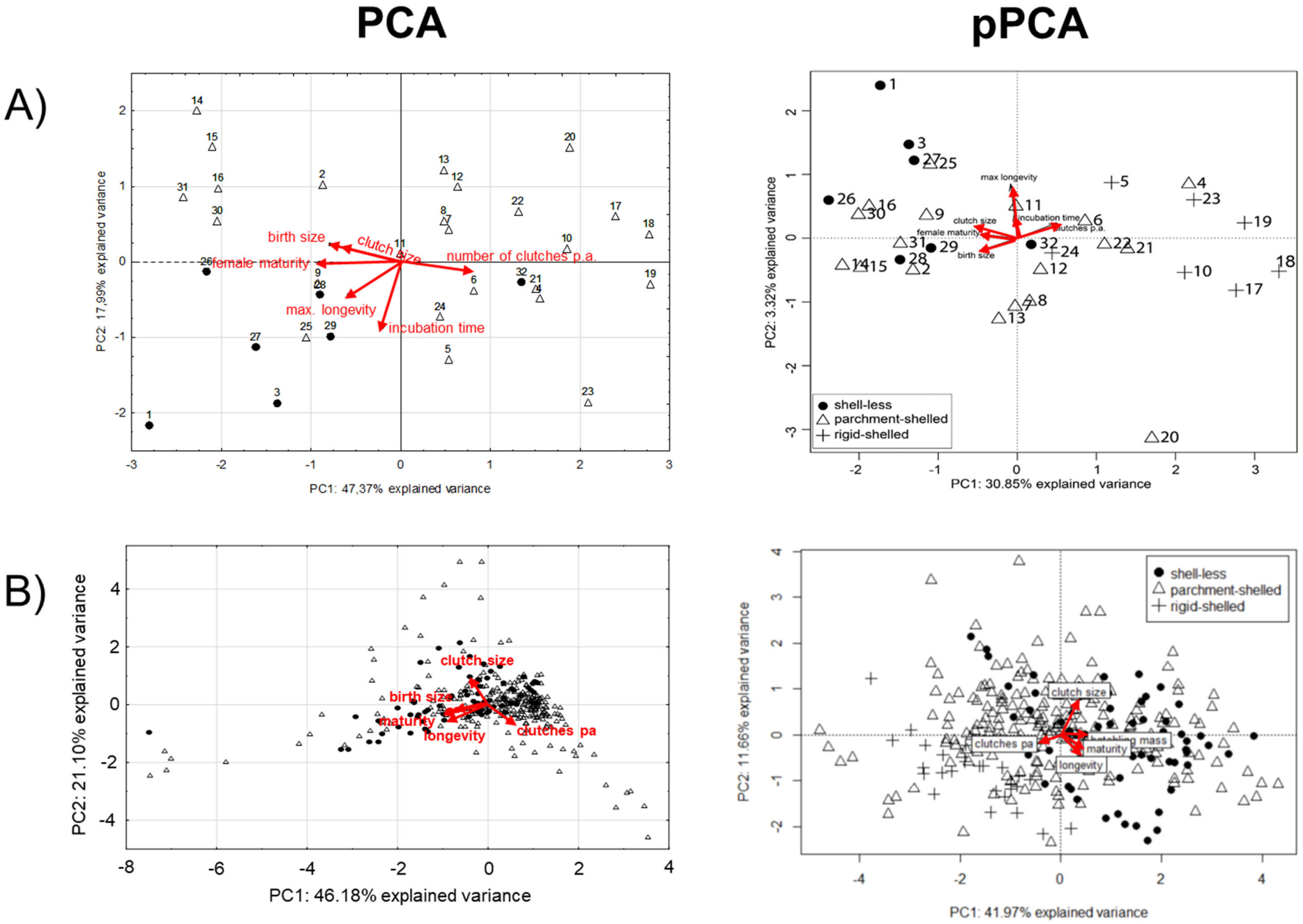
PCA
pPCA
A)
B)
PC1: 47,37% explained variance
PC2: 17,99% explained variance
birth size
clutch size
number of clutches p.a.
female maturity
max. longevity
incubation time
PC1: 30.85% explained variance
PC2: 3.32% explained variance
max longevity
clutch size
incubation time
clutches p.a.
female maturity
birth size
shell-less
parchment-shelled
rigid-shelled
PC1: 46.18% explained variance
PC2: 21.10% explained variance
clutch size
birth size
maturity
longevity
clutches pa
PC1: 41.97% explained variance
PC2: 11.66% explained variance
clutch size
clutches pa
maturity
longevity
shell-less
parchment-shelled
rigid-shelled

References Text S1.

Hallmann K, Griebeler EM (2015) Eggshell types and their evolutionary correlations with life-history strategies in squamates. PLoS ONE 10, e0138785

Klein N., Griebeler EM. (2018) Growth patterns, sexual dimorphism, and maturation modelled in Pachypleurosauria from Middle Triassic of central Europe (Diapsida: Sauropterygia), Fossil Record 21, 137-157.

Scharf I., Feldman, A., Novosolov M., Pincheira-Donoso D., Das I., Böhm M., Uetz P., Torres-Carjaval O., Bauer A., Roll U., Meiri S. (2015) Late bloomers and baby boomers: ecological drives of longevity in squamates and the tuatara. Global Ecology Biogeography 24, 396-405.

Text S2.

The growth models established in this paper on nothosaurs primarily aim at a mathematical formulation on how fast an individual had increased its size between birth and death. We used these models, which describe growth at the macroscopic level to assess important life-history traits from nothosaur specimens (size at birth, asymptotic size, asymptotic age, age at which sexual maturity is reached). We are aware of the constraint that most of our nothosaur specimens preserved a comparative small number of growth marks, which is problematic in terms of non-linear regression analysis and statistics of growth models (fig. S2). However, for many extinct taxa the growth record as preserved in bones is the only source of direct information on their growth and their paleobiology. Our results are no hard data and their interpretations are only hypotheses on extinct taxa. We are also aware of that an individual's ontogenetic growth is an autocorrelative process and that the assumption of non-independence of data (age, size) for non-linear regression analysis is violated. However, we think that statistically more complex methods modelling ontogenetic growth and thereby controlling for this autocorrelation (e.g. Lee & O'Conner 2013), will not reveal more accurate models for specimens than ours when the number of growth marks preserved in bones is already low.

To find the best growth model(s) for each nothosaur specimen we carried out a complex model fitting procedure, which is based on Griebeler *et al.* (2013) and improved in the papers Klein *et al.* (2015) and Klein & Griebeler (2016). We already successfully applied this procedure to pachypleurosaurs (Klein & Griebeler 2018). With our approach, we aimed at the technical problem that an unknown number of growth marks could be missing from the inner part of a bone (Griebeler *et al.* 2013). Our approach also explicitly tackles a technical problem described in Myhrvold (2013). It is that a growth record could only cover the exponential, quasi-linear, or asymptotic phase of growth and has no information preserved on growth acceleration and deceleration that in turn is needed for establishing a reliable sigmoidal growth model on a specimen (Klein *et al.* 2015, Klein & Griebeler 2016).

Please note that contrary to the studies of Griebeler *et al.* (2013) and of Klein & Griebeler (2016) no mass estimates were available for nothosaur specimens. This is mainly because most nothosaur humeri are only assignable at the genus level due to high ontogenetic-, intra- and interspecific variability and preservation issues (Klein *et al.* 2016). Furthermore, many taxa are only incompletely known and a reliable mass

estimation requires a humerus and femur of the same individual (Anderson *et al.* 1985; Campione & Evans 2012). Due to the poor preservation of some of the humeri (incomplete and damaged) we used midshaft width as a proxy of a specimen's humerus length and thus of its body size. All models obtained for nothosaur specimens relate midshaft width $L(t)$ (mm) to time t (years).

Growth acceleration and deceleration preserved in the growth record? To assess whether the growth record of a specimen covers only the exponential, quasi-linear, or asymptotic phase of growth (Myhrvold 2013) we fitted an exponential, linear, and asymptotic equation to its ontogenetic growth series preserved in the midshaft region of the bone. We therefore used the following equations, in which L_0 is midshaft width at the first growth mark ($t = 0$), L_{death} is midshaft width at the last growth mark preserved or observed at the outer cortex, and g the growth parameter.

Exponential growth model: $$L(t) = L_0 \exp(gt) \quad (1)$$

Linear growth model: $$L(t) = L_0 + gt \quad (2)$$

Asymptotic growth model: $$L(t) = L_0 + (L_{death} - L_0)(1 - \exp(-gt)) \quad (3)$$

Standard growth models applied to specimens. We also considered four standard growth models (Fitzhugh 1976) for each of the specimens. These were the von Bertalanffy (vBGM), Gompertz (GGM), logistic (LGM), and Chapman-Richards (CRGM) growth model. In all standard growth models t is a real number (time axis), L_0 the initial midshaft width, L_{max} the maximum width, and g the growth parameter.

The specific formulation of the vBGM that we used is based on the Pütter-von Bertalanffy equation (von Bertalanffy 1938, 1957; Pütter 1920). It has been successfully applied in this form to many extant reptile taxa (Halliday & Verrell 1988) including snakes, lizards (Shine & Charnov 1992), turtles (Frazer & Ehrhart 1985), and crocodiles (Magnusson & Sanaiotti 1995) in order to mathematically describe their ontogenetic growth in body size (i.e. snout-vent-length or total length). This asymptotic growth model formulated on gain in body length over ontogeny has no inflection point, but under a cubic transformation which is used to describe gain in body mass ($Mass = L(t)^3$) the inflection point is found at about 30% (=100*8/27) of asymptotic mass.

vBGM: $$L(t) = L_{max} - (L_{max} - L_0)\exp(-gt) \quad (4)$$

The GGM has been applied to describe length growth in extant chelonians (Andrews 1982, Hailey & Coulson 1999). In this model the inflection point is located at about 38% (=100/e) of asymptotic length and the time at which it is seen is set by parameter *i* in the specific model formulation used by us. We used the following equation to implement the GGM.

GGM: $$L(t) = L_0 + L_{max}\exp(-\exp(-g(t-i))) \quad (5)$$

The LGM has been successfully used to describe growth in smaller extant reptiles (Magnusson & Sanaiotti 1995) including tortoises (Ritz *et al.* 2010). This model has the inflection point at 50% of asymptotic length and the time at which the point is seen is set by parameter *i* in the formulation used by us. The following equation describes the LGM that we used in our study.

LGM: $$L(t) = L_0 + \frac{L_{max}}{1+\exp(-g(t-i))} \quad (6)$$

We finally considered the CRGM for each specimen. Contrary to the vBGM, GGM and LGM this model has a parameter *m*, which sets the inflection point on the length (midshaft width) axis. Parameter *i* in our formulation is again the time at which the inflection point is observed. The CRGM is able to generate any sigmoidal growth curve within the two extremes, a monotonic concave increase (no inflection point, maximum growth rate at birth) and a monotonic convex increase (no inflection point, truncated exponential model). By choosing specific values for parameter *m*, the CRGM is able to mimic the vBGM (*m*=2/3), the GGM ($m \rightarrow 1$, equation 6 is not defined for $m = 1$!), and the LGM ($m = 2$) (Richards 1959).

The formulation of the CRGM that we used is taken from Gaillard *et al.* (1997) and is based on Richards (1959), but contrary to the formulation used by these authors, ours allows for a flexible L_0.

CRGM: $$L(t) = L_0 + \frac{L_{\max}}{(1+(m-1)\exp(g(i-t)))^{1/(m-1)}} \qquad (7)$$

Please note that our formulations of the GGM (5) and LGM (6) also allow a flexible location of the inflection point with respect to an individual's age and length (midshaft width, as the CRGM). Note also that only under the vBGM the midshaft width at age 0 (midshaft width at birth) is L_0 and asymptotic width equals L_{max}. By contrast, for the GGM, LGM, and CRGM midshaft width at age 0 (at birth) is $L(t)$ evaluated at t = 0 (= $L(0)$) and asymptotic width is $L_0 + L_{max}$. Under the GGM, LGM, and CRGM parameter L_0 allows for a non-zero length at t = 0 and thus it moves the respective growth curve along the length (midshaft width) axis.

The following Figure A demonstrates the different shapes of growth curves established by our four models (4) through (7).

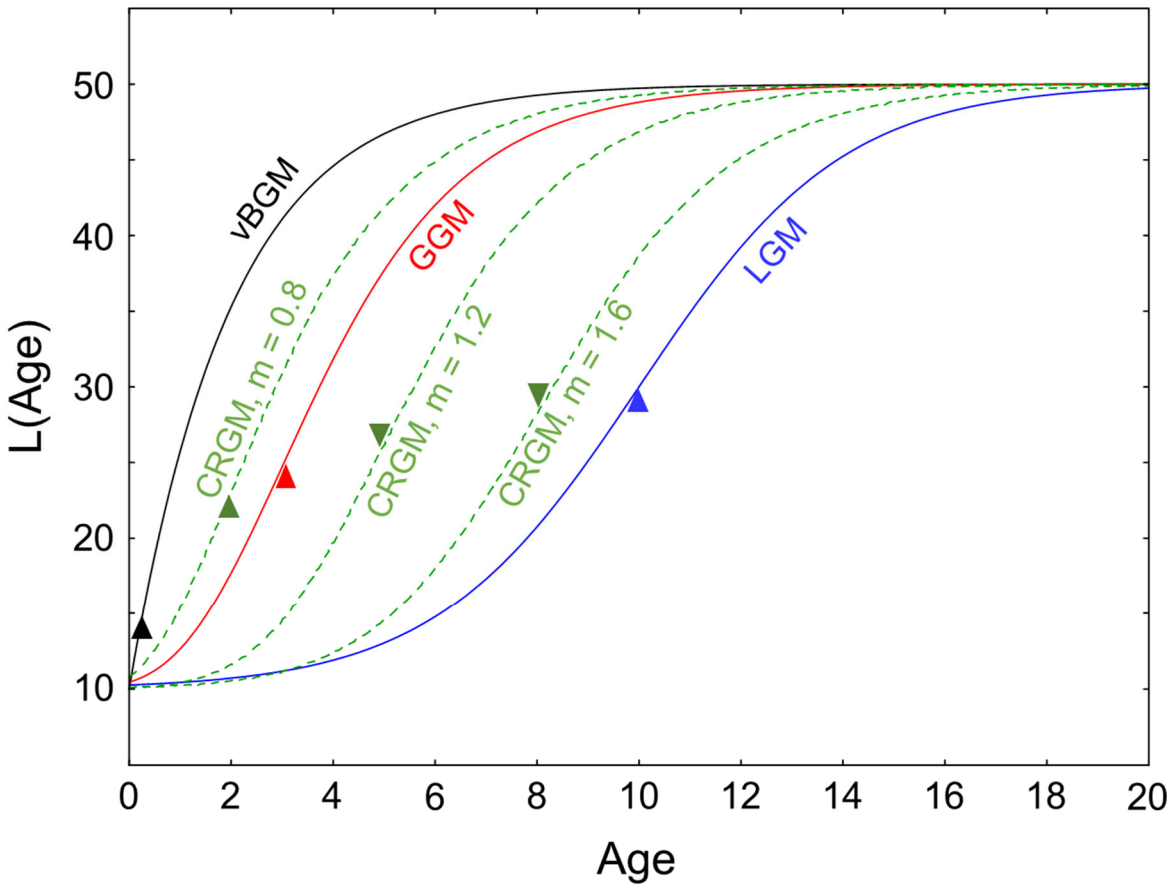

Figure A. Shapes of growth curves generated by our four models. In all growth models (equations 4 through 7), L_{birth} equals 10 length units and the asymptotic length of the individual is 50 length units. Growth parameter g equals 0.5 in all growth curves shown. Values of parameter i used by the GGM, LGM, and CRGM were estimated by eye in order to generate a growth curve for which L_{birth} ($L(0)$) equals 10 length units. Parameter i is 3 for the GGM, 10 for the LGM, 2 for the CRGM with m = 0.8, 5 for the CRGM with m = 1.2, and 8 for the CRGM with m = 1.6. Please note the large differences in sexual maturation (triangles) and in ages at which the asymptotic length is reached between models. By choosing $m > 2$ the CRGM is able to generate an even later sexual maturation and a higher age at which the individual is fully-grown than the LGM (m = 2). Triangles mark inflection points of growth curves, except for the vBGM where the age at which 30% of asymptotic mass is reached.

The number of parameters assumed by our equation on the vBGM (4) is three (L_0, L_{max}, and g), four (L_0, L_{max}, g and i) for both the GGM (5) and LGM (6), and even five (L_0, L_{max}, g, i, and m) for the CRGM (7). These high numbers can become problematic in non-linear regression analysis when the number of growth marks preserved in a bone is comparatively small as e.g. for the nothosaurs studied herein (fig. S2, table S1). We therefore additionally considered for each of these four standard growth models simpler equations. In these equations different parameters were *a priori* fixed to specific values (i.e. we did not fit them, L_0 was set to zero, L_0 equalled the midshaft width observed at the first growth mark or L_{max} was the width corresponding to the last growth mark preserved, for more details on this refer to the table below). Thus, 6 equations derived from the general equation (4) were applied to each specimen implementing von Bertalanffy growth, 11 equations implementing Gompertz growth (equation 5), 11 equations implementing logistic growth (equation 6), and 12 equations implementing Chapman-Richards growth (equation 7). Overall, for each of the specimens under study we considered in total 40 equations on standard growth models (listed below) and three equations enabling a test whether not only one growth phase is preserved in its growth record (1 through 3).

The 40 equations used to describe growth in nothosaur specimens studied. The vBGM is parameterized by parameters L_0, L_{max}, and g (equation 4), the GGM (equation 5) and LGM (equation 6) are both parameterized by parameters L_0, L_{max}, g and i, and the CRGM (equation 7) is parameterized by parameters L_0, L_{max}, g, i, and m. Starting with a full parameterisation of each of these four growth models (all model parameters are estimated), we stepwise reduced their numbers of parameters estimated (#parameters estimated) by *a priori* setting specific parameters to fixed values in the respective equation before fitting the remaining ones. est. = this parameter is estimated during the fitting process; from last gm = in the respective model equation L_{max} equals the midshaft width observed at the last growth mark or (if preserved) at the outer cortex; fixed to 0 = L_0 (or i) equals 0 in the respective model equation.

Growth model	**#parameters estimated**	L_0	L_{max}	g	i	m
vBGM	3	est.	est.	est.		
	2	est.	from last gm	est.		
	2	from first gm	est.	est.		
	2	fixed to 0	est.	est.		
	1	from first gm	from last gm	est.		
	1	fixed to 0	from last gm	est.		

GGM and LGM	4	est.	est.	est.	est.	
	3	est.	from last gm	est.	est.	
	3	from first gm	est.	est.	est.	
	3	fixed to 0	est.	est.	est.	
	2	est.	from last gm	est.	fixed to 0	
	2	from first gm	est.	est.	fixed to 0	
	2	fixed to 0	est.	est.	fixed to 0	
	2	from first gm	from last gm	est.	est.	
	2	fixed to 0	from last gm	est.	est.	
	1	from first gm	from last gm	est.	fixed to 0	
	1	fixed to 0	from last gm	est.	fixed to 0	
CRGM	5	est.	est.	est.	est.	est.
	4	est.	from last gm	est.	est.	est.
	4	from first gm	est.	est.	est.	est.
	4	fixed to 0	est.	est.	est.	est.
	4	est.	est.	est.	fixed to 0	est.
	3	from first gm	from last gm	est.	est.	est.
	3	fixed to 0	from last gm	est.	est.	est.
	3	est.	from last gm	est.	fixed to 0	est.
	3	from first gm	est.	est.	fixed to 0	est.
	3	fixed to 0	est.	est.	fixed to 0	est.
	2	from first gm	from last gm	est.	fixed to 0	est.
	2	fixed to 0	from last gm	est.	fixed to 0	est.

Estimation of the number of missing growth marks in the inner part of the bone. Many of our studied nothosaurs had large marrow cavities, which could indicate that the first growth mark preserved in these bones does not correspond to midshaft width at birth and that some growth marks are missing (resorbed, table S1). Please note that contrary to sauropods, for nothosaurs, we aimed to estimate the sizes (midshaft width) at birth of specimens. This made the two methods given in Griebeler *et al.* (2013) estimating the number of missing growth marks inapplicable to these fossils.

Both methods presented in that paper make use of a known birth size (i.e. egg mass was used as an estimate of sauropod hatchling mass in Griebeler *et al.* 2013) in order to estimate the number of missing growth marks. The method presented herein was already successfully applied to the sauropterygians *Simosaurus* (Klein & Griebeler 2016), Placodontia (Klein *et al.* 2015), and Pachypleurosauria (Klein & Griebeler 2018). To estimate for our nothosaur specimens how many growth marks could be missing in the inner part of bones (#res. gms) we first applied the method from Sander & Klein (2005) in order to have an educated guess. Then, we considered different birth sizes and numbers of missing growth marks for each of the 40 equations on standard growth models in order to find an even better estimate of the number of growth marks missing in the inner part of the bone. To implement this manual grid search on the best number of missing growth marks and the best birth size for a specimen, we generated new growth series based on those preserved in the specimen's growth record. For the number of missing growth marks we assumed one up to (3 * #res. gms) growth marks and stepwise increased this value by one growth mark. The lowest birth size (midshaft width at birth) considered was 0.1 which corresponds to the lowest annual increase in midshaft width seen across our nothosaur sample and the largest was the midshaft width preserved at the first growth mark in the specimen's growth record. Our increment in midshaft width was (midshaft width from the first growth mark) / (3 * #res. gms) for our manual grid search. In the following, we give an example on how our manual grid search was carried out in order to estimate the number of missing growth marks and birth sizes of nothosaurs.

Growth series preserved in the growth record of a hypothetical nothosaur specimen

number of the growth mark	1	2	3	4	5
midshaft width (in mm)	0.6	1.0	2.3	3.0	3.2

#res. gm = 1 (here arbitrary set to one, for fossils this educated guess is derived from the method of Sander & Klein 2005)

Tested numbers of missing growth marks = {0, 1, 2, 3} (3 = 3*1 = 3 * #res. gm)

Midshaft width at the first growth mark preserved = 0.6 (midshaft width observed at gm no. 1)

Tested birth sizes = {0.1, 0.2, 0.4, 0.6} (0.2 = 0.6 / 3*1 = "midshaft width observed at gm no. 1" / 3 * #res. gm)

All growth series examined in our manual grid search in order to find the best number of missing growth marks and birth size for our hypothetical specimen.

age	no gm missing	1 gm missing				2 gm missing				3 gm missing			
0	0.6	0.1	0.2	0.4	0.6	0.1	0.2	0.4	0.6	0.1	0.2	0.4	0.6
1	1.0	0.6	0.6	0.6	0.6								
2	2.3	1.0	1.0	1.0	1.0	0.6	0.6	0.6	0.6				
3	3.0	1.3	1.3	1.3	1.3	1.0	1.0	1.0	1.0	0.6	0.6	0.6	0.6
4	3.2	3.0	3.0	3.0	3.0	1.3	1.3	1.3	1.3	1.0	1.0	1.0	1.0
5		3.2	3.2	3.2	3.2	3.0	3.0	3.0	3.0	1.3	1.3	1.3	1.3
6						3.2	3.2	3.2	3.2	3.0	3.0	3.0	3.0
7										3.2	3.2	3.2	3.2

For this hypothetical specimen, we would have finally done 520 fits on standard growth models (= 13 growth series considering different numbers of missing growth marks and birth sizes * 40 equations on standard growth models).

Numerical model solving. All regression analyses were carried out in the free software R statistics (version 3.0.2). We applied the function "nls" from the *nls* package for model fitting. As each of our standard growth models (equation 4 through 7) has a conditional linear parameter (Ritz & Streibig 2008) we used the fitting algorithm "plinear" provided in the *nls* package to minimise residuals. This algorithm is very robust in terms of choosing starting values on model parameters, as it is classical linear regression analysis (Ritz & Streibig 2008). Starting values must not be that precise as e.g. for the Gauss-Newton algorithm that the *nls* package provides as an alternative method (Ritz & Streibig 2008). Nevertheless, when the fitting algorithm on a specific model equation did not converge for a given growth series, we additionally tried some further guesses on starting values for model parameters to be estimated. We aimed to find more support that this equation is indeed not applicable to this growth series. Please note that when using the fitting algorithm "plinear" the conditional linear parameter ".lin" is additionally estimated (Ritz & Streibig 2008). Thus, the

midshaft width at the specimen's birth (L_{birth}) equals L_0*.lin for the vBGM and $L(0)$*.lin for the GGM and LGM. Analogously, only for the vBGM the asymptotic midshaft width of the specimen (AL) equals L_{max}*.lin, whereas under the GGM, LGM, and CRGM it is ($L_0 + L_{max}$)*.lin.

Identification of candidate standard models. To identify biological reliable standard growth models from the total of equations and growth series considered for a specimen (the 520 equations considered for our hypothetical nothosaur growth series), we first discarded those for which the fitting algorithm did not converge. Next, we excluded those for which model parameter estimates (including the conditional parameter .lin) did not differ significantly from zero and then subsequently those estimating negative birth sizes or negative asymptotic sizes, having an inflection point seen at a negative age of the individual or a negative growth parameter or a larger birth size than asymptotic size (midshaft width shrinks with increasing age). Fortunately, for all nothosaurs studied the remaining number of models was very small compared to the total number of standard growth model equations and growth series on numbers of missing growth marks initially tested. For these, we finally tested whether they also passed the statistical assumptions of a non-linear regression analysis. For testing the assumption of equal variances of residuals we used Levene's test and for a test whether the residuals are normally distributed we applied the Shapiro-Wilk test (Ritz & Streibig 2008). Models passing all these filters were our candidate standard growth models for a given nothosaur specimen. Passing statistical tests on statistical assumptions of non-linear regression analysis did not kick out any model for nothosaurs, presumable as the respective null hypotheses are conservative and sample sizes were small.

Selection of the best growth model(s) for a specimen.

Since the identification process described before often revealed more than one candidate standard growth model for a nothosaur specimen studied, we identified the best model(s) out of these by an AIC based approach (Burnham & Anderson 2002). For this, we used the standard threshold $\Delta AIC \leq 10$ (Burnham & Anderson 2002). First, the best model in terms of AIC (corrected for small sample sizes) was identified, and next ΔAIC values were calculated for all others. In the case that ΔAIC of the linear model was less than 10 compared to the best candidate model (Burnham & Anderson 2002), we assumed that the growth record only covers the quasi-stationary phase of growth (Myhrvold 2013). In the case that ΔAIC of the

exponential model was less than 10 compared to the best candidate model (Burnham & Anderson 2002), we assumed that the growth record covers only the exponential phase of growth (Myhrvold 2013). In the case that ΔAIC of the asymptotic growth model was less than 10 compared to the best model (Burnham & Anderson 2002), this could either indicate the asymptotic phase of growth (Myhrvold 2013) or not. Thus, only if all other models within the ΔAIC≤10 range were sigmoidal (GGM, LGM or CRGM), i.e. not at least one vBGM equation was within the ΔAIC≤10 range, we assumed that the growth record covers only the asymptotic phase of growth (Myhrvold 2013). Please note that the vBGM (equation 4 has no inflection point) is no special case when applying our approach to mass-based growth series in order to test whether a growth record only covers the asymptotic phase of growth. In this case, the vBGM is also sigmoidal and a better fit of an asymptotic model to the growth record clearly indicates the asymptotic phase of growth. Please note that our ΔAIC≤10 model selection approach could lead to the observation that e.g. for MB.R. 282 two and five missing growth marks were plausible, while three and four seem to be not (table S1). For these specimens models assuming three or four marks passed our filtering for candidate models, but their ΔAIC values were slightly higher than 10.

Calculation of life-history traits from models.

We calculated for each specimen five life-history traits from its best growth curves (=vBGM, GGM, or LGM models within ΔAIC ≤ 10, table S1): midshaft width at birth (L_{birth}, equals L_0 * .lin for a vBGM and $L(t)$ * .lin for the GGM and LGM with $L(t)$ evaluated at time $t = 0$), asymptotic midshaft width (AL; equals L_{max} * .lin for a vBGM, and equals ($L_0 + L_{max}$) * .lin for the GGM or LGM), age at which sexual maturity is reached (ASM), midshaft width of a fully-grown individual (99% AL; 99% of asymptotic midshaft width), and age at which the individual is fully grown (AA; age at which 99% of AL is reached). To estimate the age at which the individual reached sexual maturity from its growth curve (ASM), we assumed that the inflection point of the curve coincides with sexual maturation. Evidence for this concept exists in reptiles and amphibians (Reiss 1989; Kupfer *et al.* 2004; Lee & Werning 2008; Ritz *et al.* 2010). Under the GGM, ASM is seen at about 38% of AL, and under the LGM at 50% of AL. As our formulation of the vBGM (equation 4) has only an inflection point when mass is plotted against age (it is seen at 30% of asymptotic mass), we assumed as in Klein *et al.* (2015b) and Klein & Griebeler (2018) that ASM coincides with the age at which 30% of AL is reached.

For Wijk 13-259, Wijk 10-170, Wijk 13-141, MHI 1193, SMNS 84851, SMNS 84772, and *Ceresiosaurus* for which a single standard growth model passed $\Delta AIC \leq 10$ (table S1) L_{birth}, AL, ASM, 99% AL, and AA were derived from the respective curve. To find estimates on L_{birth}, AL, ASM, 99% AL, and AA for all other specimens for which more than one growth model passed $\Delta AIC \leq 10$ (table S1) we did model averaging of trait values (Burnham & Anderson 2002). We therefore first estimated each of these five traits from all best growth curves on the specimen's growth record. We then averaged for each of the traits these values based on the models' respective Akaike weights (Burnham & Anderson 2002).

Estimated birth to adult size ratios (L_{birth}toAL) of specimens were derived from model averages of L_{birth} and 99% AL, again except for Wijk 13-259, Wijk 10-170, Wijk 13-141, MHI 1193, SMNS 84851, SMNS 84772, and *Ceresiosaurus*.

References Text S2.

Anderson JF, Hall-Martin A, Russell DA (1985) Long-bone circumference and weight in mammals, birds and dinosaurs. J. Zool. Soc. Lond. A 207, 53-61.

Andrews RM (1982) Patterns of growth in reptiles. In: Gans C, Pough FH, eds. Biology of the Repilia Vol. 13, Physiology D. New York: Academic Press. 273-320.

von Bertalanffy L (1938) A quantitative theory of organic growth. Human Biology 10, 181-213.

von Bertalanffy L (1957) Quantitative laws in metabolism and growth. Q. Rev. Biol. 32, 217-231.

Burnham KP, Anderson DR (2002) Model selection and multimodal inference: a practical information-theoretic approach. New York: Springer.

Campione NE, Evans DC (2012) A universal scaling relationship between body mass and proximal limb bone dimensions in quadrupedal terrestrial tetrapods. BMC Biology 10, 60

Fitzhugh HA (1976) Analysis of growth curves and strategies for altering their shape. J. Anim. Sci. 42, 1036-1051.

Frazer NB, Ehrhard LM (1985) Preliminary growth models for Green, *Chelonia mydas*, and Loggerhead, *Caretta caretta*, turtles in the wild. Copeia 1, 73-79.

Gaillard J-M, Pontier D, Allaine D, Loison A, Herve J-C et al. (1997) Variation in growth form and precocity at birth in eutherian mammals. Proc R Soc Lond B 264, 859-868.

Griebeler EM, Klein, N, Sander PM (2013) Aging, maturation and growth of sauropodomorph dinosaurs as deduced from growth curves using long bone histological data: An assessment of methodological constraints and solutions. PLoS ONE 8, e67012.

Hailey A, Coulson IM (1999) The growth pattern of the African tortoise *Geochelone pardalis* and other chelonians. Can J Zool 77, 181-193.

Halliday TR, Verrell PA (1988) Body size and age in amphibians and reptiles. J Herpetol 22, 253-265

Klein N, Neenan JM, Scheyer TM, Griebeler EM. (2015) Growth patterns and life-history strategies in Placodontia (Diapsida: Sauropterygia) R. Soc. Open sci. 2, 140440.

Klein N, Griebeler EM (2016) Bone histology, microanatomy, and growth of the nothosaurid *Simosaurus gaillardoti* (Sauropterygia) from the Upper Muschelkalk of southern Germany/Baden-Württemberg. C. R. Palevol. 15, 147-167.

Klein, N., Sander, P. M., Krahl, A., Scheyer, T. M. & Houssaye, A. (2016) Diverse aquatic adaptations in *Nothosaurus* spp. (Sauropterygia) – Inferences from humeral histology and microanatomy. PLoS ONE 11, e0158448.

Klein N., Griebeler EM. (2018) Growth patterns, sexual dimorphism, and maturation modelled in Pachypleurosauria from Middle Triassic of central Europe (Diapsida: Sauropterygia), Fossil Record 21, 137-157.

Lee AH, O'Conner PM (2013) Bone histology confirms determinate growth and small body size in the noasaurid theropod *Masiakasaurus knopfleri*. Journal of Vertebrate Paleontology 33, 865-876.

Magnusson WE, Sanaiotti TM (1995) Growth of Caiman crocodilus in Central Amazonia, Brazil. Copeia 2, 498-501.

Myhrvold NP (2013) Revisiting the estimation of dinosaur growth rates. PLoS ONE 8, e81917

Pütter A (1920) Wachstumsähnlichkeiten. Pflügers Archive für Gesamte Physiologie Menschen und Tiere 180, 298-340.

Richards FJ (1959) A flexible growth function for empirical use. J Exp Bot 10, 290-300.

Ritz C, Streibig JC (2008) Nonlinear regression with R. Springer, New York.

Ritz J, Griebeler EM, Huber R, Clauss M (2010) Body size development of captive and free-ranging African spurred tortoises (*Geochelone sulcata*): high plasticity in reptilian growth rates. Herpetological Journal 20, 213-216.

Sander PM, Klein N (2005) Developmental plasticity in the life history of a prosauropod dinosaur. Science 310, 1800-1802.

Shine R, Charnov EL (1992) Patterns of survival, growth and maturation in snakes and lizards. Am Nat 139, 1257-1269.

Figure S1. Phylogenetic principal component analysis (pPCA) plot from Hallmann & Griebeler (2015), but modified. It is based on the life-history traits of 32 studied squamate species and indicates one global principal component (PC1) and one local principal component (PC2). Axes are based on six life-history traits of species. Arrows indicate loadings, thus the contribution of life-history traits to PC1 and PC2. The phylogenetic weight matrix is based on the phylogeny of Pyron *et al.* (2013). In the original plot three "egg shell types" were marked, here we have only marked oviparous (hard-shelled+rigid-shelled eggs) and viviparous (shell-less eggs) species.

Squamate traits: AA=asymptotic age/maximum longevity (years), ASM=age at which sexual maturity is reached (days), $L_{hatchling}$=total length at birth (cm), clutch size=number of eggs/litter size, number of clutches per year, incubation time (days).

Species and numbers: 1. *Anguis fragilis*, 2. *Coronella girondica*, 3. *Eryx jaculus*, 4. *Eublepharis macularius*, 5. *Euleptes europaea*, 6. *Gallotia atlantica*, 7. *Gallotia galloti*, 8. *Gallotia simonyi*, 9. *Gallotia stehlini*, 10. *Hemidactylus turcicus*, 11. *Hemorrhois ravergieri*, 12. *Lacerta agilis*, 13. *Lacerta strigata*, 14. *Macrovipera lebetina*, 15. *Malpolon monspessulanus*, 16. *Natrix natrix*, 17. *Phelsuma laticauda*, 18. *Phelsuma lineata*, 19. *Phelsuma madagascariensis*, 20. *Phrynocephalus helioscopus*, 21. *Podarcis muralis*, 22. *Podarcis siculus*, 23. *Ptyodactylus hasselquistii*, 24. *Tarentola mauritanica*, 25. *Timon lepidus*, 26. *Vipera aspis*, 27. *Vipera berus,* 28. *Vipera latastei*, 29. *Vipera renardi*, 30. *Zamenis longissimus*, 31. *Zamenis situla*, 32. *Zootoca vivipara*.

Please note that the traits clutch size, number of clutches per year, and incubation time shown in this figure (black arrow) were not used in this study to identify potentially viviparous nothosaurs. Clutch sizes of nothosaurs were only assessed from their birth-to-adult size ratios in order to check whether nothosaurs being potentially viviparous due to their combination of birth size, asymptotic age, and age at maturation could also have had large clutch sizes. Number of clutches per year was not assessable from the birth to adult size ratio preserved in the nothosaur specimens. Incubation time is simply unknown for extinct nothosaurs. The shared evolutionary history of species had a much weaker effect on squamate life-history strategies than body size (figures 3 and 4a in Hallmann & Griebeler 2015), which justifies the use of non-phylogenetic-informed PCA in this study (see text S1 for a further justification).

References Figure S1.

Hallmann K, Griebeler EM (2015) Eggshell types and their evolutionary correlations with life-history strategies in squamates. PLoS ONE 10, e0138785

Pyron RA, Burbrink FT, Wiens JJ (2013) A phylogeny and revised classification of Squamata, including 4161 species of lizards and snakes. BMC Evol Biol 13, 23627680

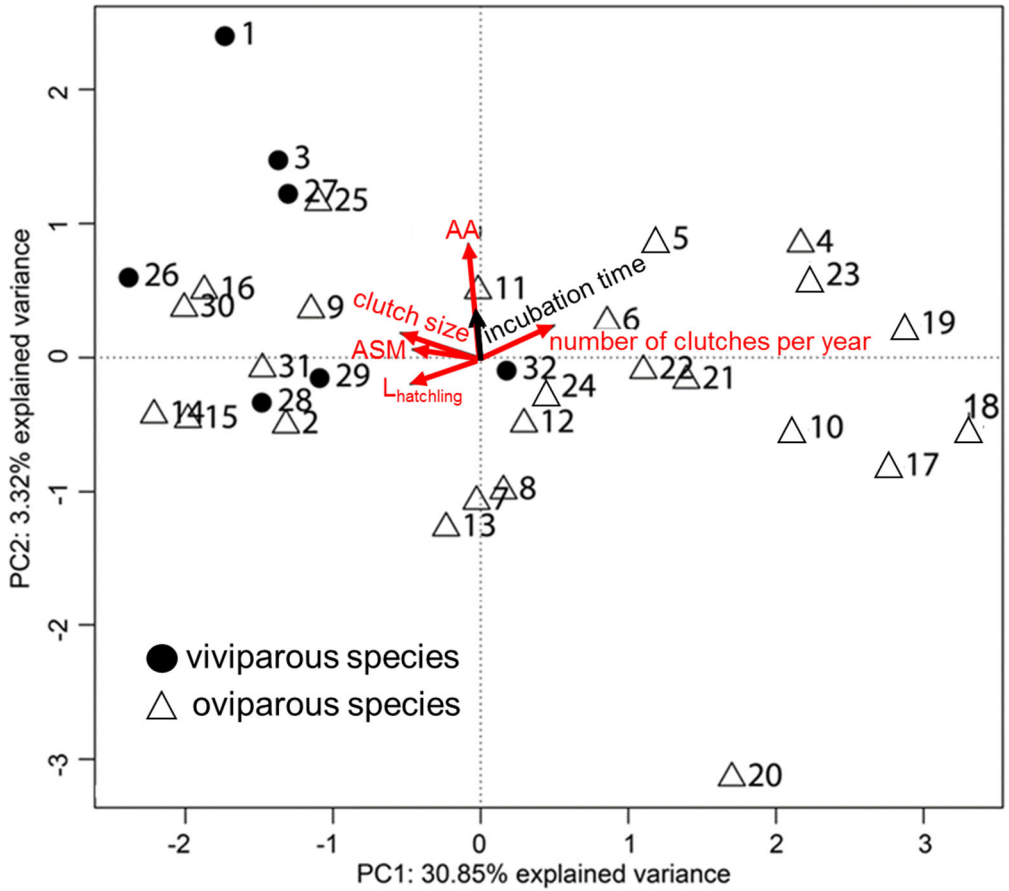

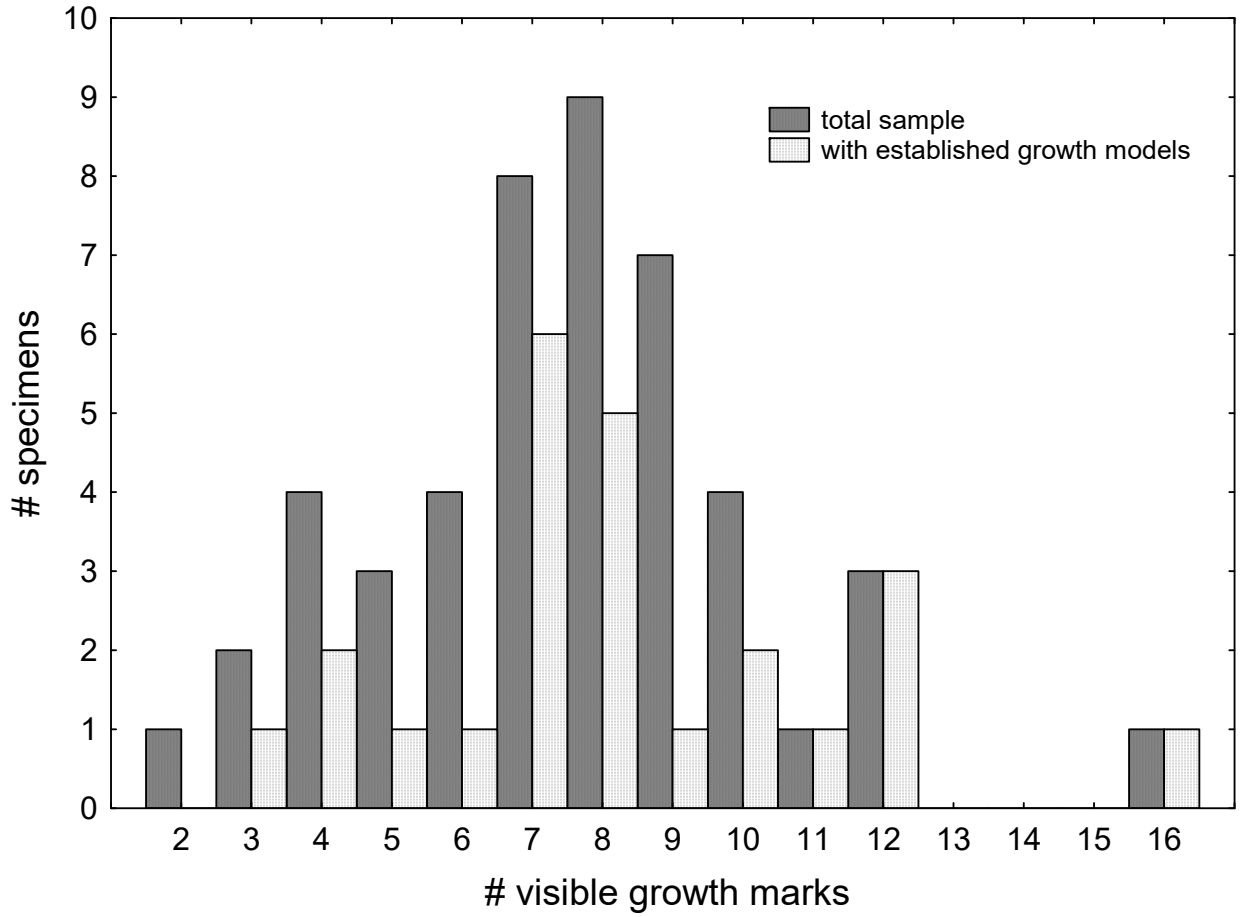

Figure S2. Numbers of visible growth marks preserved in nothosaur specimens studied. Total sample=the total nothosaur sample (47 humeri), with established growth models (24 humeri for which we were able to establish growth curves). Please note that sample sizes used for growth modelling could be larger than the number of visible growth marks, e.g. when a specimen has a hatchling line and/or an outer cortex preserved (table S1).

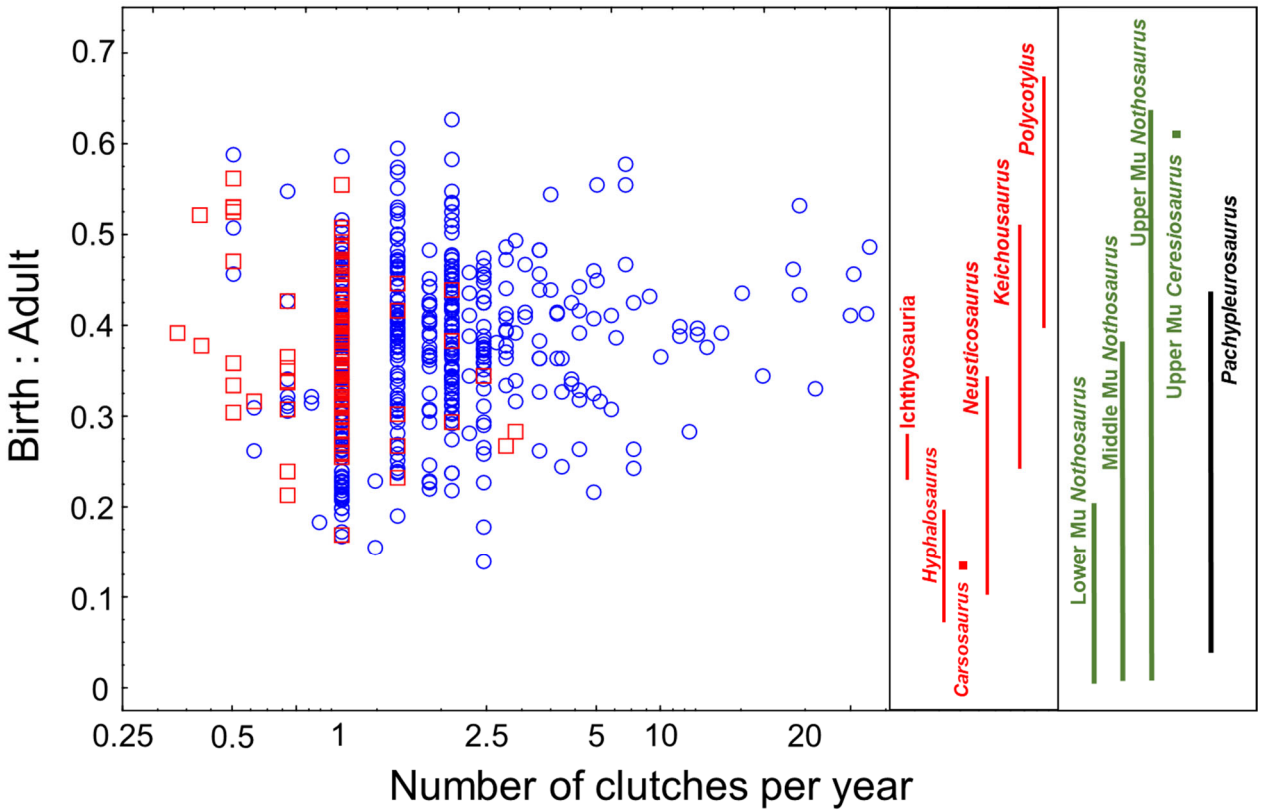

Figure S3. Birth to adult length ratios and numbers of clutches per year in extant squamates, and in viviparous fossils as well as in nothosaurs studied here and pachypleurosaurs studied by us before. Data on extant squamates are taken from Meiri *et al.* (2012, $N_{oviparous}$ = 440, $N_{viviparous}$ = 102), for data on nothosaurs, viviparous Sauropterygia and other viviparous fossil taxa please refer to table S2 and S3. Data on pachypleurosaurs are listed in table S4. Ratios of extant squamates were calculated from respective snout-vent-lengths (averages over sexes) provided by Meiri *et al.* (2012). Please note that the majority of birth to adult length ratios of viviparous fossils are underestimates, because authors measured foetuses and not neonates. For viviparous fossils, only ranges are shown. Blue = oviparous taxon, red = viviparous taxon, green = nothosaurs studied herein, black = pachypleurosaurs.

Reference Figure S3

Meiri S, Brown JH, Sibly RM (2012) The ecology of lizard reproductive output. Global Ecol. Biogeogr. 21, 592-602.

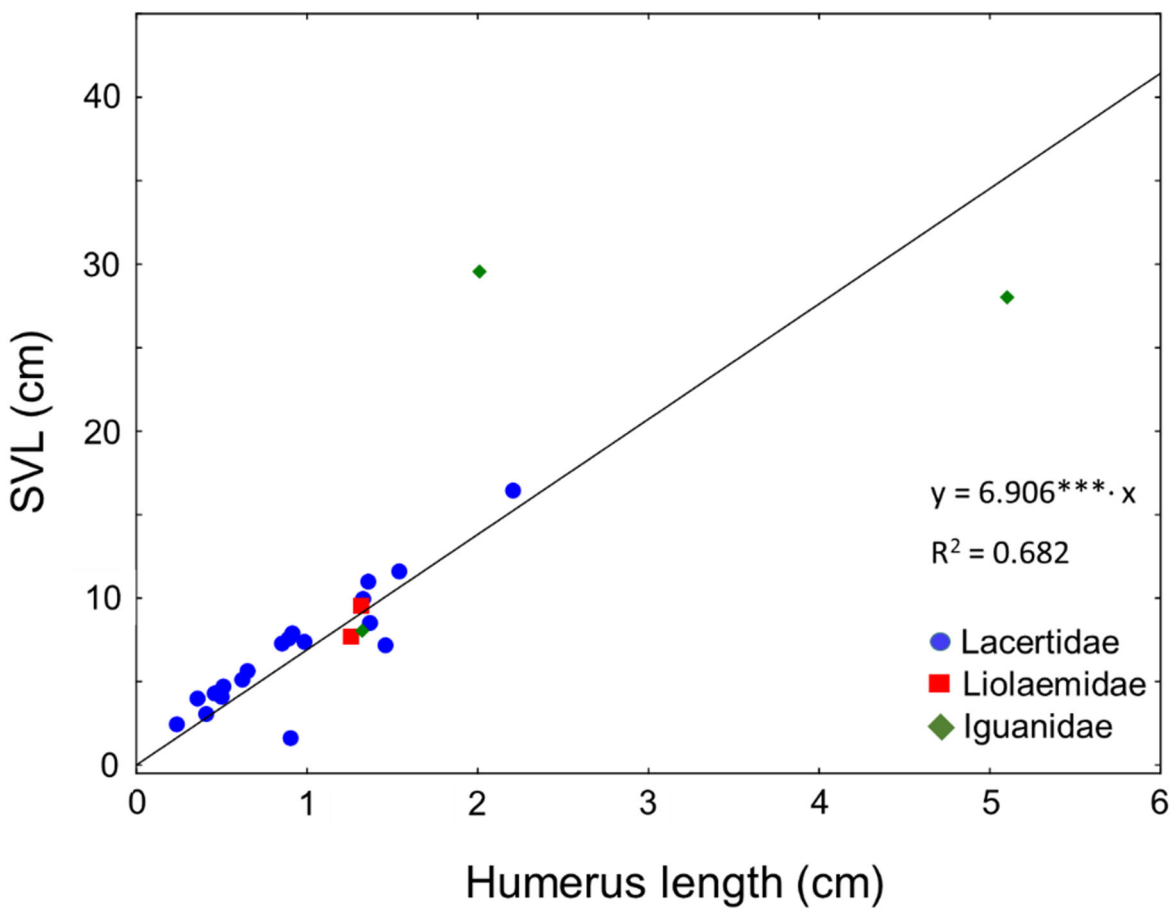

Figure S4. Correlation between humerus length and snout-vent-length. We compared in our study birth to adult length ratios of nothosaurs to those seen in viviparous fossils and in extant squamates. Ratios in nothosaurs were calculated from midshaft widths of humeri. Contrary, those used in this study on viviparous fossils were taken from literature and had been calculated from lengths of long bones and ratios of extant squamates are based on snout-vent-lengths. While midshaft width relates to long bone length, it is unclear whether humerus length relates to snout-vent-length. To test this, we measured lengths of humeri and snout-vent-lengths from skeletons of the zoological collection stored at SMNS. Individuals studied: Lacertidae (*Lacerta agilis* (N=10), *Lacerta bilineata* (N=2), *Lacerta viridis* (N=2), *Lacerta strigata* (N=1), *Podarcis muralis* (N=2), *Podarcis erhardi* (N=1), *Timon lepidus* (N=1)), Liolaemidae (*Liolaemus kuhlmanni* (N=1), *Liolaemus spec.* (N=1)) and Iguanidae (*Iguana iguana* (N=3)). Snout-vent-length (SVL) and humerus length (and thus midshaft width) correlate strongly in analysed extant squamates. *** $p < 0.001$.

Figure S5. Relationship between birth to adult size ratio and clutch size in extant squamates. Squamates taken from Scharf *et al.* (2015). Blue=oviparous squamates, red =viviparous squamates. Green lines mark birth-to-adult size ratio of nothosaurs with established growth models (tables S1 and S2). In A nothosaur specimens from the Lower Muschelkalk, in B from the Middle Muschelkalk, and in C from the Upper Muschelkalk.

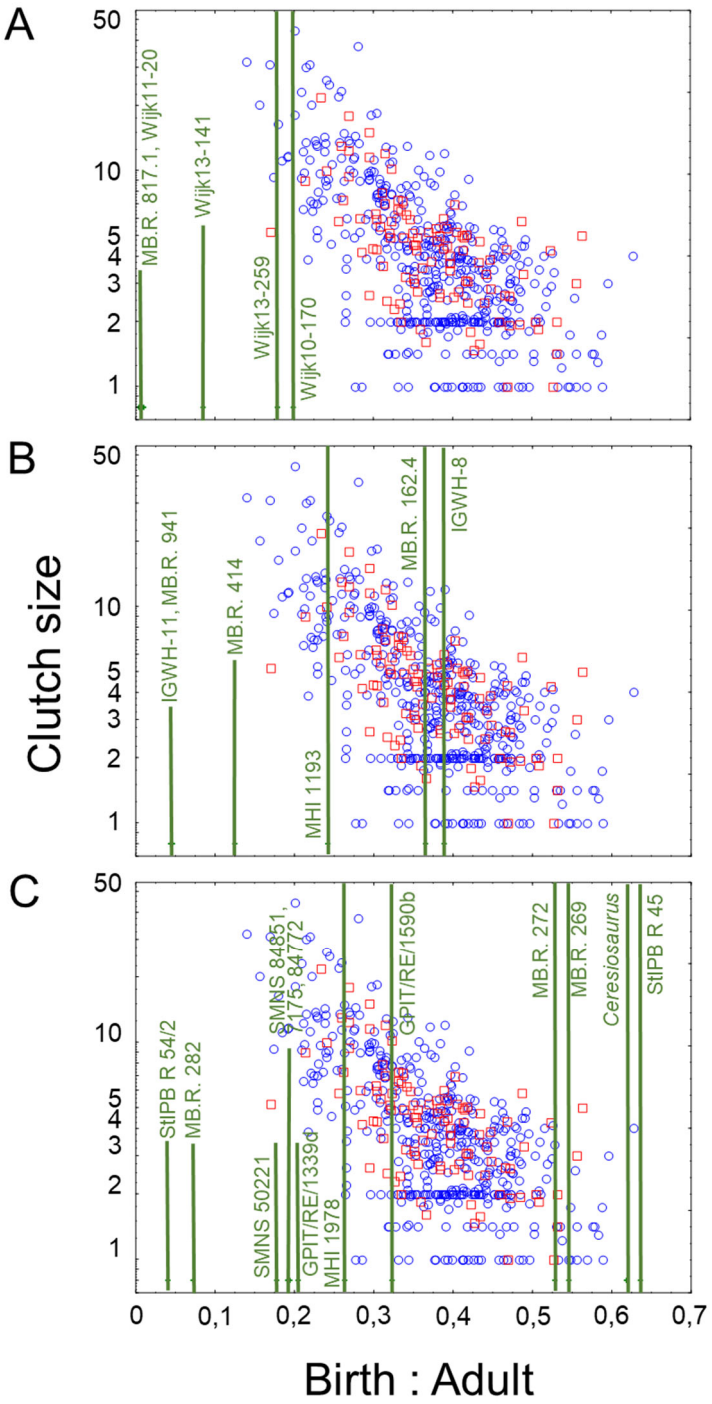

Figure S6. Growth record traced in *Nothosaurus* humeri. Arrows indicate annual growth marks. For further information on histology and microanatomy see Klein *et al.* (2016). A, Cross section of humerus Wijk13-141 under crossed nicols. B, Cross section of humerus Wijk11-20 in normal light. C, Cross section of humerus MHI 1193 under crossed nicols. D, Cross section of humerus GPIT/R/1339d under crossed nicols. A, B, and C are composite pictures of microphotographs.

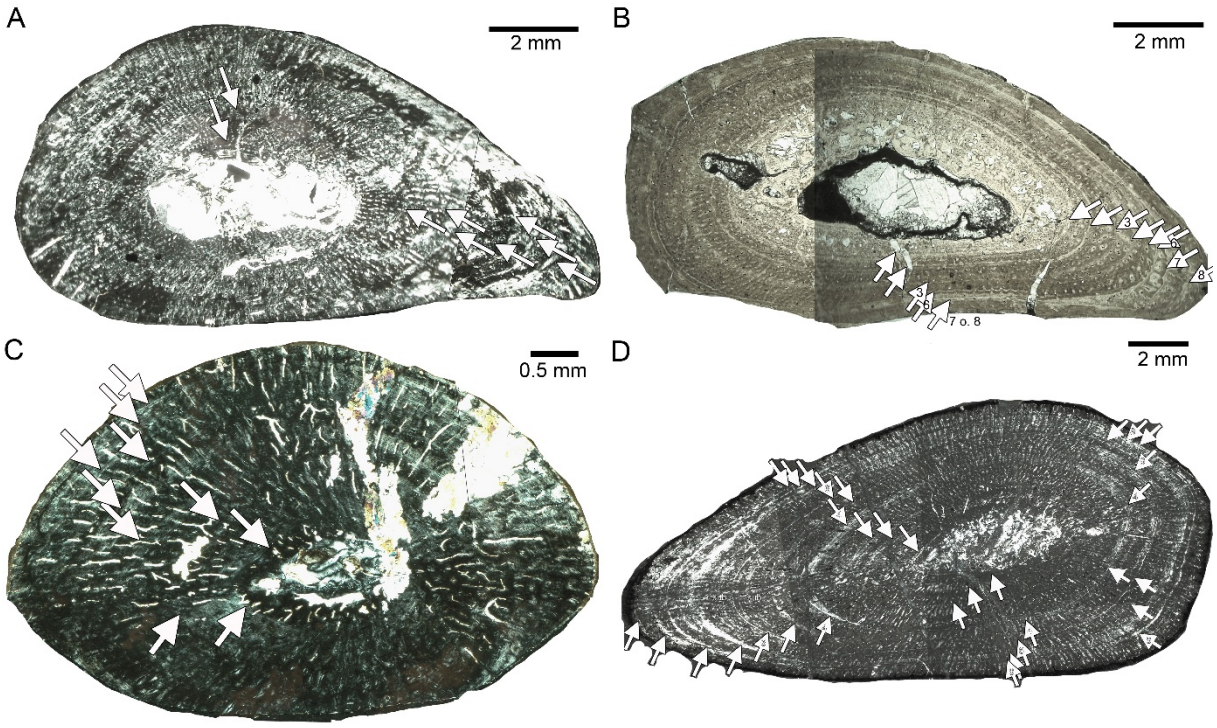

Figure S7. Growth record traced in *Nothosaurus* humeri. Arrows indicate annual growth marks. Frames indicate where in the cross section the growth record was measured. Pictures of cross sections are made with a scanner in normal light. Microphotographs are composite pictures under crossed nichols. For further information on histology and microanatomy see Klein *et al.* (2016). A1, Cross section of humerus MB.R 162.4. A2, Enlarged section where growth record was measured. B1, Cross section of humerus MHI 1978. B2, Enlarged section where growth record was measured. C1, Cross section of humerus SMNS 84851. C2, Enlarged section where growth record was measured.

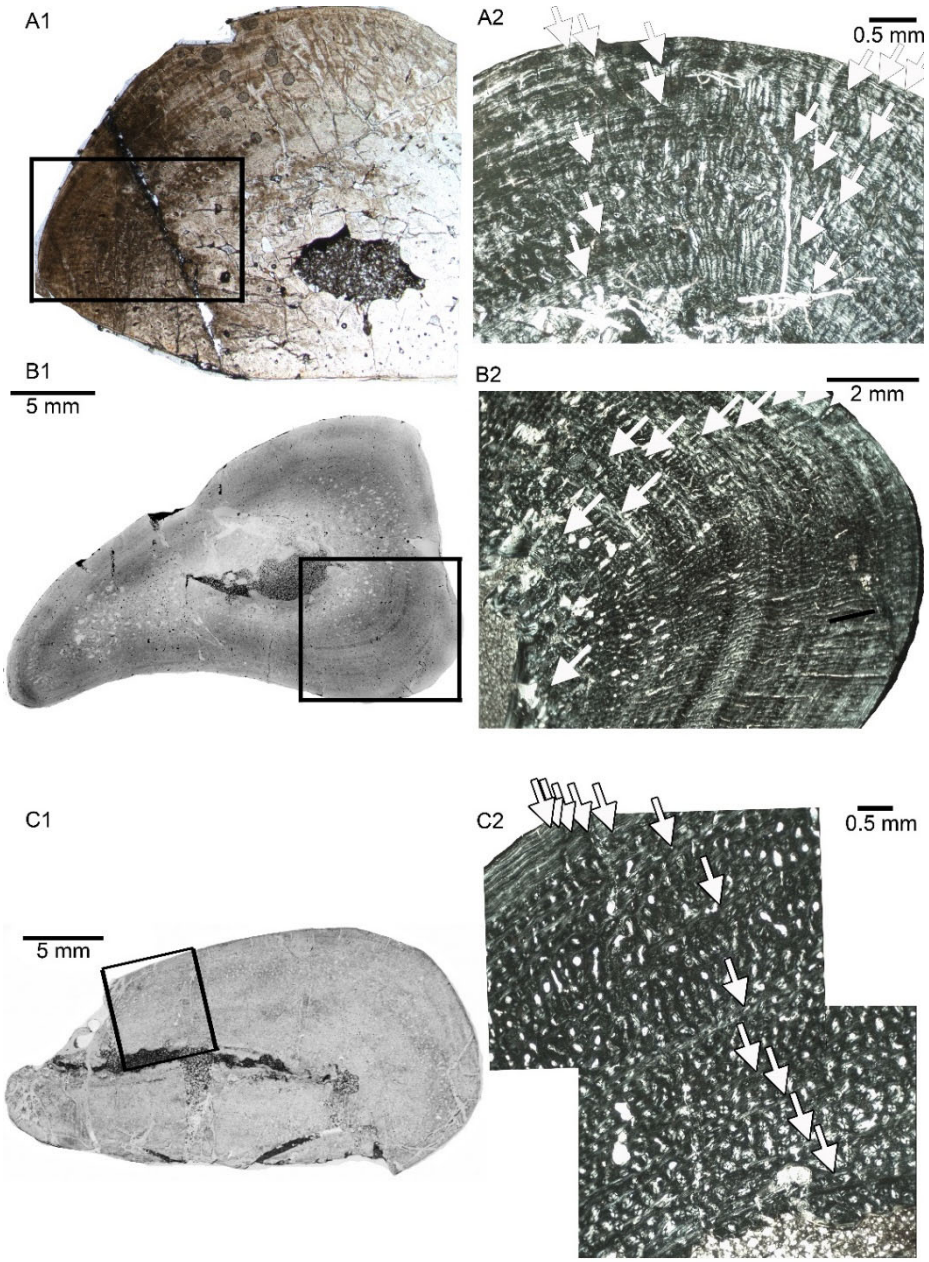

Figure S8. Growth record traced in *Nothosaurus* humeri. Arrows indicate annual growth marks. Frames indicate where in the cross section the growth record was measured. Pictures of cross sections are made with a scanner in normal light. Microphotographs are composite pictures under crossed nichols. For further information on histology and microanatomy see Klein *et al.* (2016). A1, Cross section of humerus SMNS 7175. A2, Enlarged section where growth record was measured. B1, Cross section of humerus SMNS 84772. B2, Enlarged section where growth record was measured. C1, Cross section of humerus MB. R. 272. C2, Enlarged section where growth record was measured. D1, Cross section of humerus MB. R. 282. D2, Enlarged section where growth record was measured. E1, Cross section of humerus StIPB R 45. E2, Enlarged section where growth record was measured.

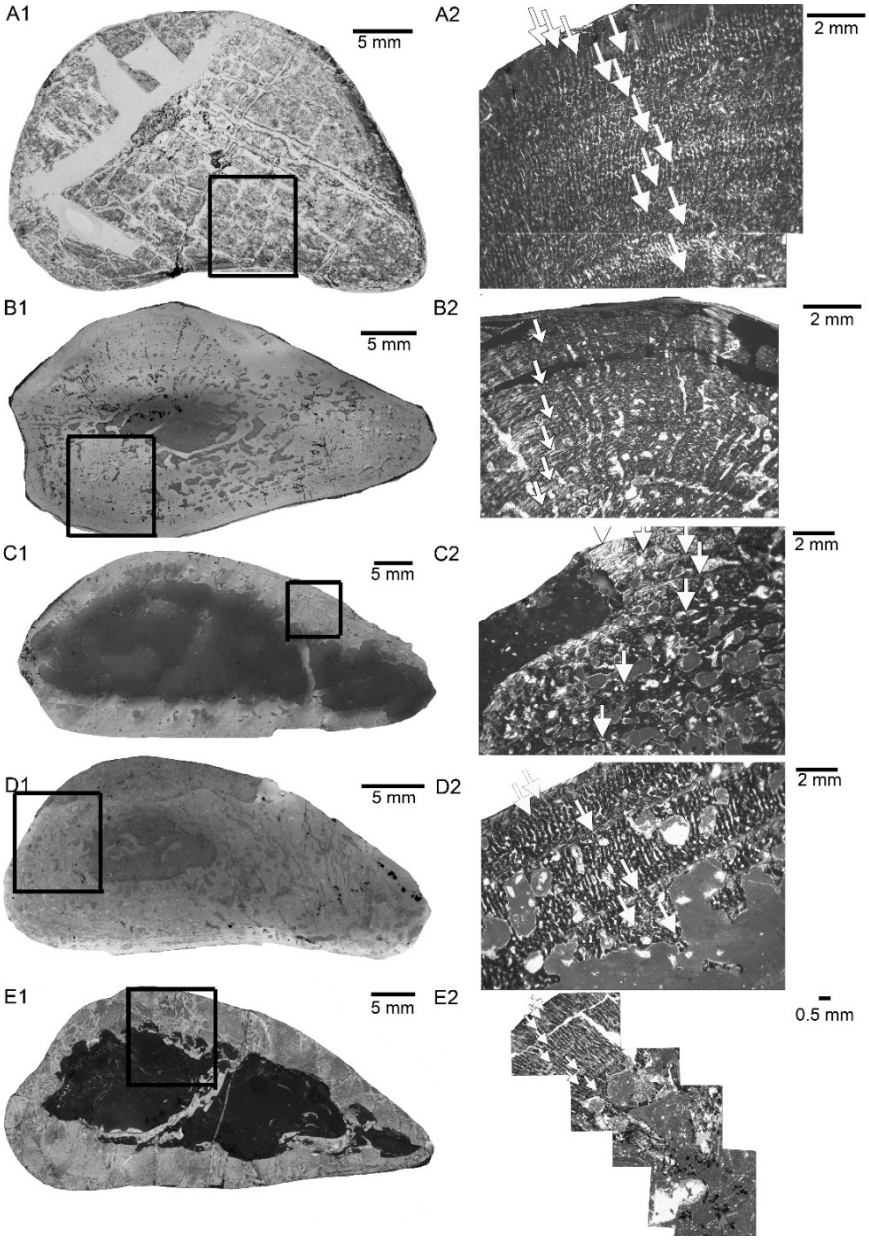

Figure S9. Growth record traced in nothosauroid humeri. Arrows indicate annual growth marks. Frames indicate where in the cross section the growth record was measured. Pictures of cross sections are made with a scanner in normal light. Microphotographs are composite pictures under crossed nichols. For further information on histology and microanatomy see Klein *et al.* (2016). A, Cross section of humerus MB.R. 269. B1, Cross section of *Ceresiosaurus* humerus (PIMUZ T4845). B2, Enlarged section where growth record was measured.

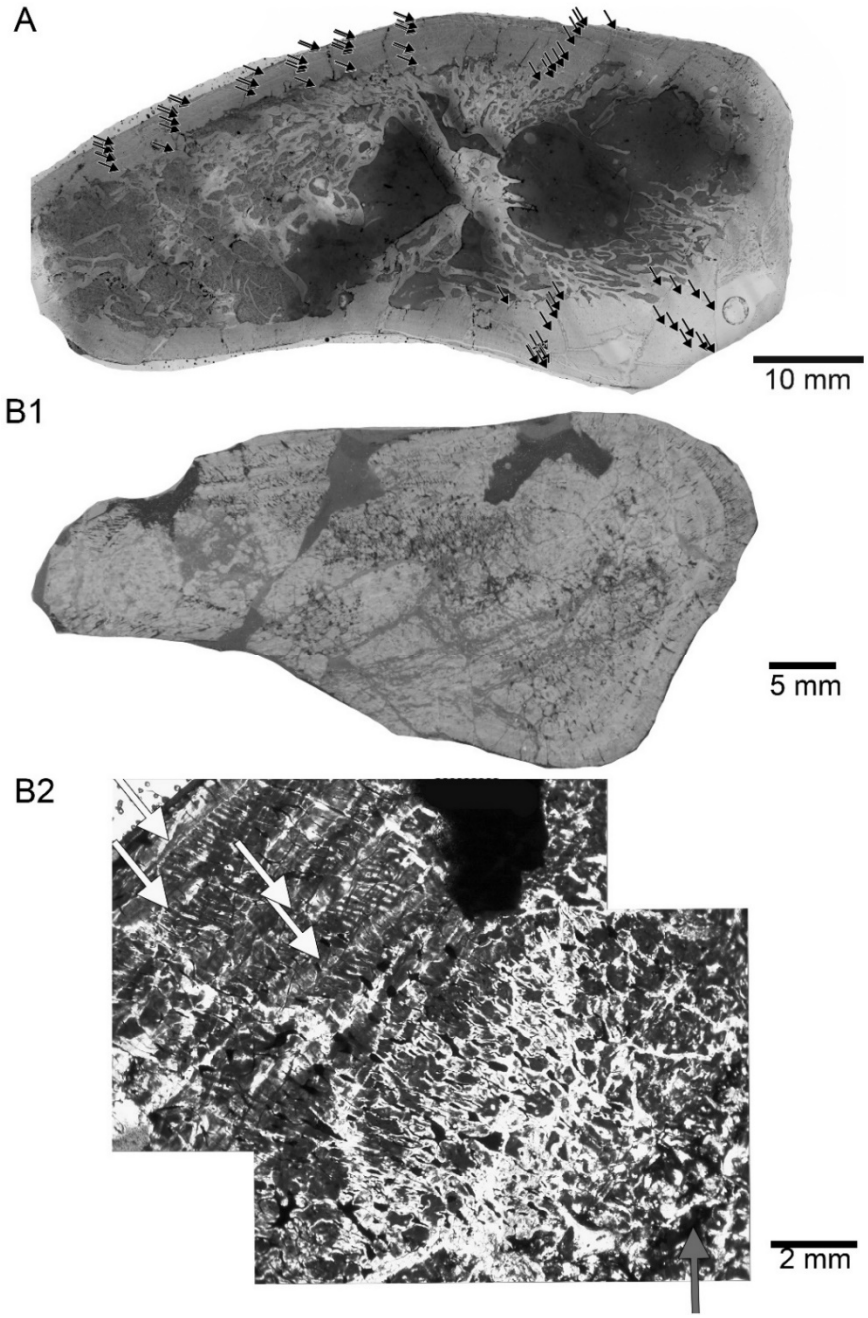

Reference Figures S6-S9
Klein, N., Sander, P. M., Krahl, A., Scheyer, T. M. & Houssaye, A. (2016) Diverse aquatic adaptations in *Nothosaurus* spp. (Sauropterygia) – Inferences from humeral histology and microanatomy. PLoS ONE 11, e0158448.

Table S1. Growth records and models for a) early Anisian (Lower Muschelkalk), b) middle to late Anisian (Middle Muschelkalk), and c) latest Anisian to early Ladinian (Upper Muschelkalk) *Nothosaurus* humeri studied. Abbreviations: mw = midshaft width used as proxy for humerus length and thus body size; bl = bone length, asterisk marks that bl is reconstructed (see methods and Klein *et al.* 2016); #visible gms = number of visible growth marks; #res. gms = number of resorbed growth marks in the inner cortex reconstructed from the method of Sander & Klein (2005); N = #visible gms + hatchling line (if visible) + outer cortex (if visible), sample size used in growth curve modelling; LM = linear model (test for quasi-linear phase of growth, Klein *et al.* 2015, Klein & Griebeler 2016); vBGM = von Bertalanffy growth model; GGM = Gompertz growth model; LGM = logistic growth model; please note that the Chapman-Richards growth model was not successfully fitted to the growth record of any of the bones; None = no model could be established, the fitting algorithm always diverged; #miss. gms = number of missing (resorbed) growth marks in the inner cortex as predicted by the growth model; L_0 = offset midshaft width in the model; width at birth is L_0 under the vBGM and *L(0)* for the GGM and LGM, L_{max} = maximum width; only for the vBGM the asymptotic width equals L_{max}, whereas under the GGM and LGM it is $L_0 + L_{max}$; g = growth parameter; i = location of the inflection point on the time axis; s.e. = standard error; res. s.e. = residual standard error of the model; AIC = AIC value of the model; df = degrees of freedom; ΔAIC = difference in the AIC value of this model and that of the best model for a specimen (Burnham & Anderson 2002); w(ΔAIC) = Akaike weight (normalised relative model likelihood, Burnham & Anderson 2002); ΔAIC(LM) = difference between the linear model and this model (test for quasi-linear phase of growth, see text S2); ΔAIC(ASY) = difference between the asymptotic model and this model (test for asymptotic phase of growth, growth decelerates only, see text St); ΔAIC(EXP) = difference between the exponential model and this model (test for exponential phase of growth, growth accelerates only, see text S2); n.a. = asymptotic/exponential model not applicable to this specimen; bold = specimen for which standard growth models (vBGM, GGM, LGM) were found, are statistically supported, biological reliable, and for which not only one phase of growth is preserved in the growth record (see text S2); p-values of estimated model parameter values * $p < 0.05$, ** $p < 0.01$, ***$p < 0.001$. For equations on growth models and identification of best models refer to text S2. Please note that model parameter i is only defined in the GGM and LGM. The abbreviation (fix) denotes in this table that in the fitted growth equation offset midshaft width L_0 was (*a priori*) manually set to zero.

Institutional abbreviations: IGWH = Institute of Geosciences of the Martin-Luther-University Halle-Wittenberg, Germany; GPIT = Paleontological collection and museum, Department Geoscience, University of Tübingen, Germany; MfN (MB.R.) = Museum of Natural History, Leibniz-Institute for Research on Evolution and Biodiversity at the Humboldt University Berlin, Germany; MHI = Muschelkalkmuseum Ingelfingen, Germany; NMNHL RGM (Wijk) = National Museum of Natural History Naturalis, Leiden, The Netherlands; PIMUZ = Paleontological Institute and Museum of the University of Zurich, Switzerland; SMNS = Stuttgart State Museum of Natural History, Germany; StIPB = Steinmann-Institute, Division of Paleontology, University of Bonn, Germany.

References Table S1

Burnham KP, Anderson DR (2002) Model selection and multimodal inference: a practical information-theoretic approach. Springer.

Klein N, Neenan JM, Scheyer TM, Griebeler EM (2015) Growth patterns and life-history strategies in Placodontia (Diapsida: Sauropterygia) R. Soc. Open sci. 2, 140440 (2015).

Klein N, Griebeler EM (2016) Bone histology, microanatomy, and growth of the nothosaurid *Simosaurus gaillardoti* (Sauropterygia) from the Upper Muschelkalk of southern Germany/Baden-Württemberg. C. R. Palevol. 15, 147-167.

Klein N, Sander PM, Krahl A, Scheyer T, Houssaye A (2016) Diverse aquatic adaptations in *Nothosaurus* spp. (Sauropterygia) – Inferences from humeral histology and anatomy. PLoS ONE 11(7): e0158448.

Sander PM, Klein N (2005) Developmental plasticity in the life history of a prosauropod dinosaur. Science 310, 1800-1802.

a) early Anisian (Lower Muschelkalk)

Bone spec. no. (mw, bl)	#visible gms (years)	#res. gms (years)	N	Model	#miss. gms (years)	L_0 (mm) s.e.	L_{max} (mm) s.e.	g ($year^{-1}$) s.e.	i (year) s.e.	Res. s.e.	df	AIC	df	ΔAIC	w(ΔAIC) (%)	ΔAIC (LM)	ΔAIC (ASY)	ΔAIC (EXP)
Wijk13-259 (6.2 mm, 43 mm*)	3	0	5	GGM	0	1.2* 0.056	5.3* 0.015	1.209* 0.053	1.3* 0.026	0.032	1	-18.2	5	0		28.2	n.a.	n.a.
Wijk13-89 (10.2 mm, 63.3 mm)	3	0	4	LM		$4.2^{n.s.}$		$1.417^{n.s.}$		1.105	2	15.4	4			0	n.a.	n.a.
Wijk10-170 (12.3 mm, 78 mm)	5	1	6	vBGM	0	2.5*** 0.368	12.8*** 0.076	0.546** 0.140		0.351	3	8.0	3	0		11.6	2.0	n.a.
Wijk13-141 (12.3 mm, 71.7 mm)	8	0	9	vBGM	0	1.9*** 0.052	22.5*** 0.191	0.086*** 0.014		0.088	6	-13.8	4	0		16.4	0	n.a.
Wijk11-265 (13.5 mm, 73 mm)	10	0	11	LM		4.1***		0.525***		0.347	9	11.7	3			0	6.5	n.a.
Wijk12-91 (14.5 mm, 86.4 mm)	5	1	6	LM		4.7**		1.265**		0.630	4	15.1	4			0	n.a.	n.a.
Wijk11-20 (14.5 mm, 95 mm)	8	2	9	vBGM	3	0.2*** 0.019	16.8*** 0.019	0.181*** 0.001		0.099	6	-14,1	4	0	81.1	22.7	2.9	n.a.
				vBGM	4	0.2*** 0.036	19.1*** 0.036	0.121*** 0.006		0.111	6	-11.2	4	2.9	19.9	19.8	0	n.a.
MB.R. 780 (42 mm, 270 mm*)	9	1-2	10	LM		22.6***		0.541*		0.922	8	19.6	3			0	n.a.	n.a.
MB.R. 817.1 (52 mm, 320 mm*)	7	2	8	vBGM	2	0.1*** 0.008	51.3*** 0.008	0.535*** 0.018		0.476	5	15.9	3	0	97.6	20.4	2.7	n.a.
				vBGM	3	0.1***	53.1***	0.361***		0.613	5	22.4	3	6.5	2.4	13.9	9.2	n.a.

b) middle to late Anisian (Middle Muschelkalk)

Bone spec. no. (mw, bl)	#visible gms (years)	#res. gms (years)	N	Model	#miss. gms (year)	L_0 (mm) s.e.	L_{max} (mm) s.e.	g ($year^{-1}$) s.e.	i (year) s.e.	Res s.e.	df	AIC	df	ΔAIC	w(ΔAIC) (%)	ΔAIC (LM)	ΔAIC (ASY)	ΔAIC (EXP)
SMNS 80154 (5.3 mm, 3.1 mm)	9	0	10	LM		1.7***		0.254***		0.194	8	-0.7	3			0	6.2	0
MHI 1193 (5.3 mm, 3.3 mm)	8	0	9	vBGM	0	1.3*** 0.039	5.3*** 0.213	0.231*** 0.039		0.054	6	-22.6	4			25.7	0	n.a.
IGWH-11 (6.6 mm,	4	1-2	5	GGM	0	0.8*** 0.183	3.5*** 0.015	0.966*** 0.111	0.363* 0.084	0.083	1	-7.3	4	7.8	1.7	13.9	1.9	n.a.
33 mm*)				LGM	0	(fix)	5.1*** 0.017	0.977*** 0.093		0.066	3	-9.5	3	5.6	5.2	16.1	0.3	n.a.
				vBGM	1	0.2*** 0.029	6.9*** 0.029	0.612*** 0.106		0.051	2	-15.1	3	0	86.6	21.7	5.9	n.a.
				GGM	2	0.2*** 0.020	6.6*** 0.020	0.852 0.079	1.7*** 0.063	0.077	1	-9.9	4	5.2	6.5	16.5	0.7	n.a.
MB.R. 162.4 (11.2 mm,	9	1-2	10	GGM	0	4.8*** 0.058	6.8*** 0.671	0.473*** 0.057	2.6*** 0.195	0.131	6	-7.4	5	0.5	46.0	21.6	13.4	n.a.
86 mm)				LGM	0	3.5*** 0.010	7.9*** 0.010	0.555*** 0.031	2.9*** 0.145	0.131	6	-7.9	4	0	54.0	22.1	13.9	n.a.
IGWH-14 (13 mm, 75 mm*)	4	1-2	5	LM		7.8***		0.796**		0.218	3	2.4	3			0	n.a.	n.a.
IGWH-7 (15.5 mm, 80.5 mm*)	9	1-2	10	LM		7.3***		0.501***		0.166	8	-3.8	3			0	n.a.	n.a.
IGWH-25 (16 mm, 76.5 mm)	6	1-2	7	LM		6.7***		0.809***		0.312	5	7.2	3			0	n.a.	n.a.
IGWH-8 (20.5 mm,	7	1	8	GGM	0	6.1*** 0.019	14.2*** 0.019	0.597*** 0.081	1.0*** 0.016	0.285	4	6.9	4	0	58.0	13.4	2.6	n.a.
98 mm*)				LGM	0	5.9*** 0.015	13.8*** 0.015	0.901*** 0.120	1.5*** 0.176	0.306	4	7.9	4	1.0	33.2	12.4	1.6	n.a.
				vBGM	1	0.3*** 0.035	20.5*** 0.035	0.420*** 0.043		0.378	5	9.8	3	3.9	8.8	10.5	-0.3	n.a.

MB.R. 539 (21 mm, 130 mm)	7	1-2	8	LM		9.0***		0.852***		0.381	6	10.0	3			0	6.9	n.a.
MB.R. 414 (27.4 mm, 145 mm*)	7	1	8	GGM	0	3.0*** 0.665	25.1*** 0.059	0.428** 0.065		0.375	5	11.3	4	0	94.4	14.8	n.a.	n.a.
				LGM	0	8.1*** 0.023	18.7*** 0.023	0.724** 0.124	1.5*** 0.271	0.535	4	16.1	4	5.6	5.6	10.0	n.a.	n.a.
MB.R. 941 (41 mm, 210 mm)	7	1	8	LGM	0	10.9*** 0.023	29.3*** 0.023	0.745*** 0.117	1.7*** 0.251	0.768	4	22.7	4	4.3	10.1	10.0	9.7	n.a.
				vBGM	1	0.2* 0.025	41.4*** 0.025	0.393*** 0.027		0.545	5	18.4	3	0	89.9	14.3	5.4	n.a.

c) latest Anisian to early Ladinian (Upper Muschelkalk)

Bone spec. no. (mw)	#visible gms (years)	#res. gms (years)	N	Model	#miss. gms (year)	L_0 (mm) s.e.	L_{max} (mm) s.e.	g ($year^{-1}$) s.e.	i (year) s.e.	Res s.e.	df	AIC	df	ΔAIC	w(ΔAIC) (%)	ΔAIC (LM)	ΔAIC (ASY)	ΔAIC (EXP)
SMNS 53012 (16.6 mm, 69.3 mm)	4	0	4	LM		7.7**		1.347***		0.156	2	-0.3	3			0	n.a.	n.a.
GPIT/RE/1339d (19 mm,	10	0	11	GGM	0	3.0***	13.9***	0.393***	3.2***	0.228	7	3.2	4	0	88.1	20.4	16.8	n.a.
						0.022	0.022	0.028	0.151									
102 mm*)				LGM	0	2.8***	13.1***	0.640***	3.9***	0.273	7	7.2	4	4.0	11.9	16.4	12.8	n.a.
						0.017	0.017	0.048	0.166									
GPIT/RE/1590b (19 mm,	7	0	7	GGM	0	4.9***	15.6***	0.994***	0.8***	0.101	3	-9.8	4	0	98.6	37.2	n.a.	n.a.
						0.005	0.005	0.046	0.005									
85 mm*)				LGM	0	4.9***	15.3***	1.466***	1.2***	0.171	3	-1.3	4	8.5	1.4	28.7	n.a.	n.a.
						0.008	0.008	0.119	0.065									
SMNS 2557 (22.8 mm, 112.2 mm)	6	0	7	LM		3.7**		1.476***		0.528	5	14.6	3			0	n.a.	n.a.
MHI 633 (25 mm, >56 mm)	2	0	3	LM		8.7***		3.3***		0.132	1	-1.6	3			0	n.a.	n.a.
MHI 1978 (28.3 mm,	11	?1	12	vBGM	0	9.9***	37.7***	0.101***		0.226	9	2.9	4	0	98.7	24.9	0	n.a.
						0.966	1.095	0.012										
183 mm)				GGM	0	8.0***	22.1***	0.276***	2.7***	0.324	8	11.6	4	8.7	1.3	16.2	8.7	n.a.
						0.019	0.019	0.020	0.225									
SMNS 17214 (29.3 mm, 160 mm*)	9	1-2	10	LM		21.4***		0.530***		0.581	8	21.3	3			0	n.a.	n.a.
SMNS 50221 (30 mm,	8	1-2	9	GGM	0	8.0***	22.4***	0.515***	1.4***	0.303	5	8.4	4	0.1	45.0	21.7	1.0	n.a.
						0.014	0.014	0.042	0.115									
152.5 mm)				LGM	0	7.8***	21.8***	0.760***	2.0***	0.437	5	15.0	4	6.7	1.6	15.1	5.6	n.a.
						0.015	0.015	0.081	0.172									
				vBGM	1	0.2***	31.4***	0.329***		0.432	6	15.3	3	7.0	1.4	14.8	5.9	n.a.
						0.028	0.028	0.024										
				vBGM	2	0.2***	36.3***	0.187***		0.370	6	12.3	3	4.0	6.4	17.8	2.9	n.a.
						0.049	0.049	0.015										
				GGM	3	0.2***	30.8***	0.417***	3.2***	0.295	5	8.3	3	0	45.6	21.8	1.1	n.a.

						0.021	0.021	0.031	0.089								
StIPB R 54/2	12	3-4	12	GGM	0	5.9***	27.0***	0.307***		0.342	9	12.8	4	0.8	24.6	27.7	n.a.	n.a.
(32 mm,						0.615	0.843	0.026										
>115mm)				LGM	0	(fix)	35.2***	0.350***		0.343	10	12.2	3	0.2	34.2	28.3	n.a.	n.a.
							0.015	0.028										
				vBGM	3	0.2***	34.2***	0.202***		0.331	9	12.0	3	0	38.2	28.5	n.a.	n.a.
						0.016	0.016	0.008										
				GGM	5	0.2***	32.3***	0.314***	4.1***	0.391	8	17.0	4	5.0	3.0	23.5	n.a.	n.a.
						0.016	0.016	0.024	0.146									
MHI 754	8	1	9	LM		13.0***		1.474***		0.448	7	14.8	3			0	n.a.	n.a.
(33.5 mm,																		
180 mm*)																		
SMNS 84851	16	0	17	LGM	0	5.1***	30.5***	0.679***	4.2***	0.391	13	17.1	4			38.0	28.5	n.a.
(35.4 mm,						0.010	0.010	0.037	0.102									
180 mm*)																		
SMNS 84772	12	1	13	vBGM	0	9.5***	49.5***	0.089***		0.192	10	-1.4	4			29.4	0	n.a.
(35.8 mm,						0.132	0.953	0.009										
165 mm)																		
SMNS 7175	12	0	13	vBGM	0	7.1***	53.0***	0.099***		0.614	10	28.8	4	2.3	23.6	22.6	0	n.a.
(38.9 mm,						0.308	0.633	0.014										
210 mm*)				GGM	0	7.1***	33.2***	0.308***	3.4***	0.563	9	26.5	4	0	73.9	24.9	-2.3	n.a.
						0.017	0.017	0.154	0.017									
				vBGM	1	0.1***	48.4***	0.124***		0.694	10	33.3	3	6.8	2.5	18.1	4.5	n.a.
						0.051	0.051	0.009										
MB.R. 279	8	3-4	9	LM		27.6***		1.063***		0.397	7	12.7	3			0	n.a.	n.a.
(42 mm,																		
236 mm*)																		
MB.R. 282	7	1	8	vBGM	0	5.0*	48.1*	0.293**		0.901	5	25.3	4	0.3	21.1	18.9	n.a.	n.a.
(42 mm,						0.681	1.847	0.053										
236 mm*)				GGM	0	5.2***	36.3***	0.725**	1.5***	0.979	4	26.6	4	1.6	10.9	17.6	n.a.	n.a.
						0.031	0.031	0.107	0.145									
				LGM	0	5.0***	35.2***	1.096**	2.0***	1.407	4	32.4	4	7.4	0.6	11.8	n.a.	n.a.
						0.036	0.036	0.217	0.218									
				vBGM	1	0.2***	59.4***	0.165**		1.303	5	34.0	3	9.0	0.3	10.2	n.a.	n.a.
						0.216	0.216	0.042										
				GGM	1	0.2***	42.2***	0.624***	2.1***	0.798	4	25.8	4	0.8	16.0	18.4	n.a.	n.a.
						0.031	0.031	0.066	0.109									
				LGM	1	0.2***	40.2***	0.999***	2.7***	1.202	4	33.2	4	8.2	0.4	11.0	n.a.	n.a.

						0.034	0.034	0.143	0.168								
				GGM	2	0.2***	42.4***	0.606***	3.1***	0.763	4	25.0	4	0	23.8	19.2	n.a.	n.a.
						0.032	0.032	0.066	0.108									
				LGM	2	0.2***	40.6***	0.936***	3.7***	1.057	4	30.9	4	5.9	1.3	13.3	n.a.	n.a.
						0.032	0.032	0.124	0.157									
				GGM	5	0.2***	42.4***	0.606***	6.1***	0.763	4	25.0	4	0	23.8	19.2	n.a.	n.a.
						0.032	0.032	0.066	0.108									
				LGM	5	0.2***	40.8***	0.908***	6.7***	1.017	4	30.2	4	5.2	1.8	14.0	n.a.	n.a.
MB.R. 278 (45 mm, 250 mm*)	9	4-5	9	LM		28.1***		1.175***		0.665	7	21.9	3			0	n.a.	n.a.
StIPB R 45 (47 mm,	8	3-4	9	GGM	0	29.7***	18.0***	0.565***	2.3***	0.266	5	6.4	5	1.4	33.6	20.1	11.7	n.a.
						3.987	0.918	0.074	0.184									
>115 mm)				LGM	0	27.6***	19.6***	0.742***	2.6***	0.246	5	5.0	5	0	66.4	21.5	13.1	n.a.
						4.915	1.551	0.106	0.221									
MB.R. 281 (48 mm, 270 mm*)	6	1-2	7	LM		24.2***		2.226***		0.770	5	19.9	3			0	n.a.	n.a.
PIMUZ AIII-1 (50.5 mm, >225 mm)	8	3-4	9	LM		38.7***		0.804***		0.257	7	4.7	3			0	n.a.	n.a.
Ceresiosaurus PIMUZ 4845 (53 mm, 232 mm)	4	0	5	LGM	0	23.1***	34.0***	0.639**	0.9*	0.151	1	-1.3	4			10.9	n.a.	n.a.
						0.016	0.016	0.040	0.154									
MHI 873 (54 mm, 290 mm*)	8	2-3	8	LM		33.1***		1.736***		0.797	6	22.8	3			0	n.a.	n.a.
SMNS 80688 (54 mm, 290 mm*)	5	1-2	6	LM		23.6***		3.457***		0.972	4	20.3	3			0	n.a.	n.a.
MB.R. 270 (55.5 mm, 350 mm)	9	2-3	10	LM		31.2***		1.787***		0.521	8	19.1	3			0	n.a.	n.a.
MB.R. 272 (56 mm,	6	2-3	6	GGM	0	36.3*	35.6*	0.751*	1.7*	0.496	2	12.0	5	2.0	26.6	10.0	n.a.	n.a.
						4.990	0.057	0.154	0.170									
305 mm*)				LGM	0	32.7*	37.6*	1.027*	1.9**	0.418	2	10.0	5	0	73.4	12.0	n.a.	n.a.

						5.529	0.064	0.200	0.177									
SMNS 81988 (57.5 mm, 310 mm*)	7	1-2	8	LM		31.2***		1.920***		0.859	6	24.0	3			0	5.5	n.a.
SMNS 17882 (57.8 mm, 320 mm*)	10	1-2	11	LM		37.7***		1.302***		1.588	9	45.2	3			0	8.0	n.a.
MB.R. 269 (74 mm,	10	2-3	11	GGM	0	43.5***	34.6***	0.439**	3.9***	0.647	7	24.5	5	7.6	3.2	10.0	n.a.	n.a.
						5.536	2.037	0.075	0.231									
400 mm)				LGM	0	42.0***	35.0***	0.708***	4.4***	0.461	7	17.8	5	0	96.8	16.7	n.a.	n.a.
						4.350	0.027	0.086	0.152									

Table S2. Life-history traits and birth to adult length ratios derived from best growth models for 24 *Nothosaurus* specimens from the early Anisian to late Ladinian (Middle Triassic; lithostratigraphical units: Lower Muschelkalk, Middle Muschelkalk and Upper Muschelkalk). For three out of the five specimens from the Lower Muschelkalk one standard growth model was clearly statistically supported, whereas for the other two specimens at least two models fitted similar well in terms of AIC. For the Middle Muschelkalk (except for one humerus) and for the Upper Muschelkalk (except for two humeri), at least two models always obtained a similar AIC support for each of the specimens studied. Thus, the majority of estimates on life-history traits of all specimens were model averages. Abbreviations: mw = midshaft width used as proxy for humerus length and thus body size; bl = bone length, asterisk marks that bl is reconstructed (Klein *et al.* 2016); bl_{birth} = bone length at birth, estimated from bl and L_{birth}toAL; vBGM = von Bertalanffy growth model; GGM = Gompertz growth model; LGM = logistic growth model; average = values of traits and of ratios are averages from best standard growth models and calculated based on their Akaike weights (table S1); L_{birth} = midshaft width at birth; AL = asymptotic midshaft width; bl_{AL} = bone length corresponding to AL, ASM = age at which sexual maturity is reached (age at which 30% of AL is reached for vBGM, inflection point for GGM and LGM); %99 AL = 99% of AL; AA = asymptotic age, estimated as age at which 99% of AL is reached; L_{birth}toAL = birth to adult midshaft width/bone length ratio. For models on specimens and their parameter values refer to table S1. Institutional abbreviations: IGWH = Institute of Geosciences of the Martin-Luther-University Halle-Wittenberg, Germany; GPIT = Paleontological collection and museum, Department Geoscience, University of Tübingen, Germany; MfN (MB.R.) = Museum of Natural History, Leibniz-Institute for Research on Evolution and Biodiversity at the Humboldt University Berlin, Germany; MHI = Muschelkalkmuseum Ingelfingen, Germany; NMNHL RGM (Wijk) = National Museum of Natural History Naturalis, Leiden, The Netherlands; PIMUZ = Paleontological Institute and Museum of the University of Zurich, Switzerland; SMNS = Stuttgart State Museum of Natural History, Germany; StIPB = Steinmann-Institute, Division of Paleontology, University of Bonn, Germany.

	Bone spec. no.	mw (mm)	bl (mm)	model	L_{birth} (mm)	bl_{birth} (mm)	AL (mm)	bl_{AL} (mm)	ASM (years)	99% AL (mm)	AA (years)	L_{birth}toAL
Lower Mu	Wijk13-259	6.2	43*	GGM	1.2	8.0	6.5	45.1	1.3	6.4	5.0	0.178
	Wijk10-170	12.3	78	vBGM	2.5	16.1	12.8	81.2	0.2	12.7	8.0	0.198
	Wijk13-141	12.3	71.7	vBGM	1.9	11.0	22.5	131.2	3.1	22.3	52.5	0.084
	Wijk11-20	14.5	95	average	0.2	1.0	17.4	114.0	2.1	17.2	27.8	0.009
	MB.R. 817.1	52	320*	average	0.1	1.0	51.5	316.9	0.7	51.0	9.0	0.003
Middle Mu	MHI1193	5.3	3.3	vBGM	1.3	0.9	5.3	3.3	0.4	5.2	18.8	0.242
	IGWH-11	6.6	33*	average	0.3	1.5	6.6	33.0	0.6	6.5	7.3	0.044
	MB.R. 162.4	11.2	86	average	4.2	32.2	11.5	88.3	2.7	11.4	10.8	0.365
	IGWH-8	20.5	98*	average	7.8	37.3	20.1	96.1	1.2	19.9	7.7	0.388
	MB.R. 414	27.4	145*	average	3.5	18.4	28.1	148.7	0.5	27.8	10.3	0.124
	MB.R. 941	41	210	average	1.9	9.7	41.3	211.5	1.0	40.9	11.3	0.046
Upper Mu	GPIT/RE/1339d	19	102*	average	3.4	18.3	16.7	89.7	3.2	16.5	14.0	0.204
	GPIT/RE/1590b	19	85*	average	6.6	29.5	20.5	91.7	0.8	20.3	5.1	0.322
	MHI 1978	28.3	183	average	9.9	63.9	37.6	243.1	0.5	37.2	42.2	0.263
	SMNS 50221	30	152.5	average	5.5	27.9	31.0	157.6	2.3	30.7	12.8	0.177
	StIPB R 54/2	32	>115	average	1.6	>5.7	39.7	>142.7	1.2	39.3	17.3	0.040
	SMNS 84851	35.4	180*	LGM	6.8	34.6	35.6	181.0	4.1	35.2	10.7	0.191
	SMNS 84772	35.8	165	vBGM	9.5	44.0	49.5	228.1	1.6	49.0	49.3	0.193

SMNS 7175	38.9	210*	average	8.3	44.8	43.5	234.8	3.1	43.1	24.6	0.191
MB.R. 282	42	236*	average	3.1	17.4	43.5	244.4	2.3	43.1	9.4	0.071
StIPB R 45	47	>115	average	30.1	>73.6	47.4	>115.9	2.5	46.9	7.9	0.635
MB.R. 272	56	305*	average	37.4	203.6	70.8	385.6	1.9	70.1	6.1	0.528
MB.R. 269	74	400	average	43.5	226.8	77.0	416.2	4.4	76.2	9.8	0.545
Ceresiosaurus PIMUZ 4845	53	232	LGM	35.3	154.4	57.1	249.9	0.9	56.5	7.3	0.618

References Table S2

Klein N, Sander PM, Krahl A, Scheyer T, Houssaye A (2016) Diverse aquatic adaptations in *Nothosaurus* spp. (Sauropterygia) – Inferences from humeral histology and anatomy. PLoS ONE 11(7): e0158448.

Table S3. Information on birth to adult size ratios and clutch sizes of fossil taxa for which viviparity is inferred from or documented in the fossil record.

Reptile subclade	Taxon	Age	Ratio (%)	Litter size	Reference	Humerus lengths (HL, cm)
Sauropterygia	*Neusticosaurus*	Middle Triassic	29	≥ 1	Sander (1989)	
			25 - 52		Sander (1988)	hatchling (HL = 0.43)
						female (HL = 0.83; HL = 1.73)
Sauropterygia	*Keichousaurus*	Middle Triassic	27; 33	4; ≥ 6	Cheng *et al.* (2004)	
			10; 11; 12; 13			Female with foetuses (HL = 1.35; HL = 1.27)
						Foetus (HL = 0.14; HL = 0.15; HL = 0.16)
Sauropterygia	*Lariosaurus*	Middle Triassic	26	4	Renesto *et al.* (2003)	
Sauropterygia	*Polycotylus*	Late Cretaceous	≥ 40; 67	≥ 1	O'Keefe & Chiappe (2011)	
Ichthyosauria	*Mixosaurus*	Middle Triassic	28	≥ 1	Brinkmann (1996)	
Ichthyosauria	*Stenopterygius*	Early Jurassic	23	≥ 1	Böttcher (1990)	
Choristodera	*Hyphalosaurus*	Early Cretaceous	≤20; 8	≤ 18	Ji *et al.* (2010)	Female (HL = 1.6)
						Foetus (HL = 0.12)
Mosasauroidea	*Carsosaurus*	Late Cretaceous	15	≥ 4	Caldwell & Lee (2001)	

References Table S3.

Böttcher R (1990) Neue Erkenntnisse über die Fortpflanzungsbiologie der Ichthyosaurier (Reptilia). Stuttgarter Beitr Nat B 164: 1-51.

Brinkmann W (1996) Ein Mixosaurier (Reptilia, Ichthyosaurier) mit Embryonen aus der Grenzbitumenzone (Mitteltrias) des Monte San Giorgio (Wchwiez, Kanton Tessin). Eclogae Geol Helv 89: 1321-1344.

Caldwell MW, Lee MSY (2001) Live birth in Cretaceous marine lizards (Mosasauroidae). Proc Roy Soc Lond B 268: 2397-2401.

Cheng Y-N, Wu X-C, Ji Q (2004) Triassic marine reptiles give birth to live young. Nature 432. 383-386.

Ji Q, Wu X, Cheng Y (2010) Cretaceous choristoderan reptiles gave birth to live young. Naturwissenschaften 97: 423-428.

O'Keefe FR, Chiappe LN (2011) Vivipary and K-selected life history in a Mesozoic marine plesiosaur (Reptilia, Sauropterygia) Science 333: 870-873.

Renesto S, Lombardo C, Tintori A, Danini G (2003) Nothosaurid embryos from the Middle Triassic of northern Italy: an insight into viviparity of nothosaurs? J Vertebr Paleontol 23: 957-960.

Sander PM (1988) A fossil embryo from the Middle Triassic Alps. Science 239: 780-783.

Sander PM (1989) The pachypleurosaurids (Reptilia: Nothosauria) from the Middle Triassic of Monte San Giorgio (Switzerland), with the description of new species. Phil Trans R Soc Lond B 325: 561-670.

Table S4. Life-history traits and birth to adult length ratios derived from best growth models established for pachypleurosaur specimens studied in Klein & Griebeler (2018). For two out of the thirteen humeri only one standard growth model was statistically supported, whereas for all others at least two models fitted similar well in terms of AIC. Abbreviations: bl = bone length; model: LGM = logistic growth model, average = values of traits and ratios are averages from best standard growth models and calculated based on their Akaike weights; L_{birth} = bone length at birth; AL = asymptotic bone length; ASM = age at which sexual maturity is reached; %99AL = 99% of AL; AA = asymptotic age, estimated as age at which 99% of AL is reached; AD = age at death; L_{birth}toAL = birth-to-asymptotic length ratio.

Institutional abbreviations: MfN (MB.R.) = Museum of Natural History, Leibniz-Institute for Research on Evolution and Biodiversity at the Humboldt University Berlin, Germany; NMNHL RGM (Wijk) = National Museum of Natural History Naturalis, Leiden, The Netherlands; SMNS = Stuttgart State Museum of Natural History, Germany; PIMUZ (T, phz) = Paleontological Institute and Museum of the University of Zurich, Switzerland.

	Bone spec. no.	bl (mm)	model	L_{birth} (mm)	AL (mm)	ASM (years)	99%AL (mm)	AA (years)	L_{birth}toAL
Dactylosaurus	MB.R. 786	44.0	average	9.1	44.8	1.5	44.3	9.1	0.220
	MB.R. 776.2	27.3	average	12.1	54.4	3.2	53.9	13.5	0.222
Anarosaurus	Wijk 09-472	43.5	average	17.1	44.1	0.4	43.7	6.3	0.387
	Wijk 07-70	44.0	LGM	16.7	45.0	1.7	44.5	5.3	0.362
	Wijk 09-58	49.00	average	13.9	50.0	1.5	49.5	5.3	0.278
aff. *N. pusillus*	SMNS 92125	18.1	average	5.7	18.0	0.5	16.6	4.6	0.341
	SMNS 50372c	17.2	average	5.0	18.4	0.1	18.2	13.4	0.272
N. pusillus	T 4178	17.5	average	8.1	17.8	0.5	17.7	8.4	0.465
	T 4211	16.5	average	3.6	16.6	0.7	16.4	10.8	0.217
N. edwardsii	T 4758	28.7	LGM	9.3	28.0	1.0	27.8	9.6	0.333
	phz 153	39.7	average	8.8	65.2	2.8	64.8	43.0	0.136
Serpianosaurus	T 4510	30.0	average	4.0	44.6	3.9	44.1	57.6	0.091
	T 119	21.3	average	1.5	21.9	3.2	21.6	15.8	0.064

Reference Table S4.

Klein N., Griebeler EM (2018). Growth patterns, sexual dimorphism, and maturation modelled in Pachypleurosauria from Middle Triassic of central Europe (Diapsida: Sauropterygia), Fossil Record 21, 137-157.